UCLA
UCLA Electronic Theses and Dissertations

Title

Quantitative Analysis of Human Facial Expression: Moving Towards The Creation of a Virtual Patient

Permalink

https://escholarship.org/uc/item/6m022427

Author

Lee, Sungah

Publication Date

2017

Peer reviewed|Thesis/dissertation

UNIVERSITY OF CALIFORNIA

Los Angeles

Quantitative Analysis of Human Facial Expression: Moving Towards The Creation of a

Virtual Patient

A thesis submitted in partial satisfaction

of the requirements for the degree

Master of Science in Oral Biology

by

Sungah Lee

2017

ABSTRACT OF THE THESIS

Quantitative Analysis of Human Facial Expression: Moving Towards The Creation of a

Virtual Patient

by

Sungah Lee

Master of Science in Oral Biology

University of California Los Angeles, 2017

Professor Won Moon, Co-Chair

Professor Sotirios Tetradis, Co-Chair

Background: Recent introduction of three dimensional facial images allows us to have access to more information than ever before, creating the potential for more accurate facial evaluation. In orthodontic diagnostics and treatment planning, facial soft tissue analysis has been broadly recognized as a critical factor leading to successful orthodontic treatment outcomes. Even though facial soft tissue is by nature dynamic data and facial expressions are the dynamic movement of these facial soft tissue, 2D static photos have been used in facial analysis in orthodontics. Our overall objective is to develop an innovative method to quantifies the dynamic movements of soft tissue in 3D during facial expressions, which could further not only orthodontics field but also other health care fields.

Methods: Dynamic system to quantify 3D facial soft tissue movement was explored through investigation into physics and mathematical modeling. 3dMD facial images of 29 participants at

five different time points (T_1, T_2, T_3, T_4, T_5) during smiling were collected from starting of each facial expression till the end. Smiling patterns were classified and only homogenous samples were finally included. 3D meshes were processed for vertex correspondence, and 28 landmarks were tracked. Data analyses were performed via MATLAB. Average smiling faces at five different time points were generated. Average displacement vectors between each time point were computed, producing the average smiling movement trajectories. Statistical p values of all landmarks in three-dimension were computed to show the significance level of displacement. Color-coded displacement vector p maps were generated for movement of each landmark over the 5 time points.

Results: 3D meshes of 10 participants at five different time points (T_1, T_2, T_3, T_4, T_5) while smiling were finally included in our study. 28 landmarks were quantitatively tracked and analyzed. Average smiling faces at five time points, average displacement vectors between each time point, and statistical p values of all landmarks in 3D were generated. Average movement trajectory while smiling was generated. Corner of lip showed maximum displacement of 6.42 mm (p<~ 0.01) in upward and outward directions. Statistically Significant displacements were shown at most landmarks of oral regions (p<0.05) rather than landmarks of nasal, eye, or eyebrow regions between each time point.

Conclusion: This is the first study to demonstrate that dynamic 3D movements of facial expressions can be quantitatively tracked and analyzed, offering an added dimension to the diagnosis and treatment planning of patients. This new approach which can allow us to analyze patients' facial expressions in three dimension would shift the diagnostic paradigms currently used in craniofacial analysis, that is, 2D static facial analysis, towards an ever progressive direction, that is, dynamic 3D facial expression analysis.

The thesis of Sungah Lee is approved.

Ki-Hyuk Shin

Reuben Kim

Won Moon, Committee Co-Chair

Sotirios Tetradis, Committee Co-Chair

University of California, Los Angeles

2017

TABLE OF CONTENTS

Introduction

When it comes to expressing emotions, members of widely different cultures have much in common. If people from various countries see a happy, smiling face of a person, they usually agree in their interpretation. They also tend to concur over surprise, sadness, anger, fear, disgust, contempt, and joy. Ekman classified facial expression patterns into 6 different categories (Anger, Fear, Surprise, Disgust, Happiness, Sadness) [1]. Today, the smile is easily the most recognized facial expression, used to convey a sense of compassion and understanding. The smile may well be the corner stone of social interaction, and many researches have classified smiling patterns in different ways.

According to Rubin, there are three smiling styles: "Mona Lisa" smile, "Canine" smile, and "Full Denture" smile. It is known that "Mona Lisa" smile is the most common style, seen in approximately 67% of the population. In this smile, the corners of the mouth are first pulled up and outward, followed by the levators of the upper lip contracting to show the upper teeth. The "Canine" smile, also called as "cuspid" smile is found in 31% of the population. The shape of the lips are commonly visualized as a diamond. This smile pattern is identified by the dominance of the levator labii superioris. They contract first, exposing the cuspid teeth, then the corners of the mouth contract to pull the lips upward and outward. The "Full Denture" smile, also called as "complex" smile characterizes 2% of the population. In this smile, the levators of the upper lip, the levators of the corners of the mouth, and the depressors of the lower lip contract simultaneously, showing all the upper and lower teeth concurrently [2]. In addition, according to Philips, there are four stages (Stage I, Stage II, Stage III, and Stage IV) and five types of smiles based on where dental and/or periodontal tissues are displayed in the smile zone [3].

It is also known that facial expression has important effects on a person's life, being critical in social interaction. In addition, human emotions are known to be recognized by analyzing facial expressions. There have been many researches regarding how to analyze smile, the most recognized facial expression. There has been a software application developed by MIT Media Lab., which can analyze our own smile and compare it with others and even can tell whether the smile captured is showing happiness or the result of frustration [4][5].

Since the fact that human emotions could be read via analysis of facial expression patterns, people in marketing field have shown great interest in this field because they recognize that emotion drives brand loyalty and purchase decisions. However, traditional way of measuring emotional response such as surveys and focus groups has created a gap by requiring viewers to think about and say how they feel. Even though neuroscience provides insight into how the mind works, it typically requires expensive and bulky equipment and lab type settings which limit the use. However, companies like Affectiva, a start-up company spun out of the MIT Media Lab., have been working on a software called Affedex that trains computers to recognize human emotions based on their facial expressions. Affedex reads facial expressions to measure the emotional connection people have with advertising, brands, and media [5].

Interestingly, children with repaired cleft lip are known to have abnormal nasolabial movements. For example, children with repaired unilateral cleft lip do not have symmetrical nasolabial movements. They exhibit abnormal puckering patterns and the cleft side rises when they smile. Given the important effects that facial expression has on a person's life, if we could document the patterns of facial expression in patients with repaired cleft lip, this analysis would help clinicians to modify primary labial repair. In addition, in facial paralysis reconstruction, it is necessary to understand the facial movements during normal smile, that is, the direction and

extent of movement because techniques of facial paralysis reconstruction which apply forces to the mouth mimic the vectors of movement on the patients' normal side. However, dynamic mimetic motions are difficult to assess. Even though there have been quite a few studies regarding smiling patterns, those were using "static" measurement techniques [6][7][8].

Facial soft tissue analysis has evolved over time. There have been advances in analyzing facial soft tissue with the latest advancements in technology such as three dimensional (3D) photographic imaging, creating the potential for more comprehensive facial evaluation. However, up to this point, current evaluation of facial expression such as smile, which is the dynamic movement of 3D facial soft tissue, relies largely on subjective visual evaluation and 2D point to point static distance from 2D static photos, not giving an accurate information about the patients' facial expression patterns [6][7][8]. To our knowledge, there have been no studies investigating in how to quantitatively analyze the dynamic movements of soft tissue in three dimension during facial expressions.

The immediate objectives of this project strive to develop the method which can quantify the dynamic 3D movements of soft tissues while facial expressions are being made. This research will open the door to the 3D dynamic analysis, where changes in facial 3D soft tissues could be quantitatively tracked and analyzed over time during facial expressions.

Accomplishing our goal would result in the first new approach for dealing with the dynamic movements of soft tissues in 3D, adding another dimension to the facial analysis in the health care field. Application of this new technology would allow dynamic soft tissue movement (facial expressions) diagnostics for treatment planning in various health care specialties (i.e. orthodontics, oral/maxillofacial and plastic surgery). Completion of this dynamic facial expression analysis in 3D would dramatically change the diagnostic paradigms currently used in

craniofacial analysis, that is, 2D static facial analysis, towards a totally new and progressive direction, that is, dynamic 3D facial expression analysis.

Overall Objectives and Specific Aims

2D static photos have been used in facial analysis in orthodontics. Our overall objective is to develop an innovative method to quantifies the dynamic movement of soft tissue in 3D during facial expressions, which could further not only orthodontics field but also other health care fields. This new approach can offer an added dimension to the diagnosis and treatment planning of patients.

In orthodontics diagnostics and treatment planning, facial soft tissue analysis has been broadly recognized as a critical factor, leading to successful orthodontic treatment outcomes. However, facial soft tissue is by nature dynamic data, and facial expression is the dynamic movement of these facial soft tissue. Therefore, it is important to know how to deal with dynamic movement of the facial soft tissue, which has never done before.

With the advances of three-dimensional photography systems (i.e. 3dMD), three-dimensional facial photographs of patients in orthodontic practice has become available. Research has demonstrated that three-dimensional imaging modalities have increased accuracy compared to traditional imaging modalities, trying to develop new analyses which could allow their application in clinical use [1] [2]. However, up to this point, this valuable 3dMD data couldn't be well utilized due to the lack of the method to analyze.

Current evaluation of facial expression relies largely on subjective visual evaluation and 2D point to point static distance from 2D static photos, not giving an accurate information about the patients' facial expression patterns. To our knowledge, there have been no studies

4

investigating in how to quantitatively analyze the dynamic movements of soft tissue in three dimension during facial expressions [6].

Therefore, one of our immediate goal is to use our orthodontic department's 3dMD Imaging System to quantify dynamic movement of 3D facial soft tissues. Ultimately, this research project will contribute to the creation of a dynamic three-dimensional movement trajectory of facial expressions and establishment of a new method to quantitatively track and analyze the changes in soft tissues in 3D while facial expressions are being made. Overall, this study seeks to advance static 2D facial analysis into dynamic 3D facial expression analysis by aiming to:

1. Find mathematical models to describe moving objects (motion), and find a set of functions to quantify the movement of landmarks. Link and sync the sets of functions as one entity.

2. Find a method to process 3D dynamic data in an organized and efficient way, develop a protocol to quantitatively track and analyze the dynamic movement of all landmarks in 3D between each time point.

3. Average 3dMD face models at each time point, yielding the average landmarks at each time point, then compute average displacement vectors between each time point.

4. Develop a new approach to compute p values in 3D, yielding color-coded displacement vector p maps between each time point.

5. Visualize dynamically the average smiling movement trajectory.

Accomplishing our goal would result in the first new approach for dealing with the dynamic movements of soft tissues in 3D, adding another dimension to the facial analysis in the health care field. Application of this new technology would allow dynamic soft tissue movement (facial expressions) diagnostics for treatment planning in various health care specialties (i.e. orthodontics, oral/maxillofacial and plastic surgery). Completion of this dynamic facial expression analysis in 3D would dramatically change the diagnostic paradigms currently used in craniofacial analysis, that is, 2D static facial analysis, towards a totally new and progressive direction, that is, dynamic 3D facial expression analysis.

Background / Significance

It is known that facial expression has important effects on a person's life, being critical in social interaction. Today, the smile is easily the most recognized facial expression, used to convey a sense of compassion and understanding. Considering the fact that facial expressions have critical roles in social interaction, there have been many researches regarding how to analyze smile, resulting in many applications in various fields [2][3]. Not only facial expressions are critical in social interaction, but also by analyzing facial expression patterns, we can recognize human emotions. For example, there has been a software application developed by MIT Media Lab., which can analyze our own smile and compare it with others, and can tell whether the smile is showing happiness or the result of frustration [4] (Figure 1).
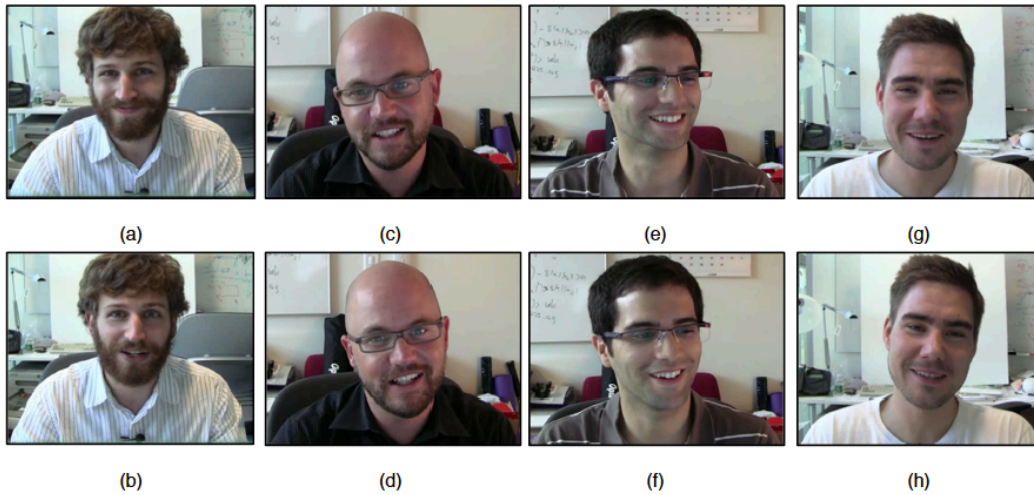
Figure 1: (Adapted from Hoque et al. [4]) Four participants, each smiling while being in either a (i) frustrated or (ii) delighted state. Can you tell which smile is which state? (a), (d), (f), (h) are taken from instances of frustration; (b), (c), (e), (g) are from instances of delight.

Quantitative analysis of facial expressions can have a tremendous influence in health care field. For example, to successfully reconstruct smile in the patients with facial paralysis, an understanding of the facial movements during a normal smile is necessary. Techniques of facial paralysis reconstruction apply forces to the mouth and these forces mimic the vectors of movement on the patients' normal side, allowing a symmetrical smile reconstruction [6][7][8]. Given the important effects that facial expression has on a person's life, if we could quantitatively analyze the patterns of facial expression in patients, this analysis would help clinicians in diagnosis and treatment planning, improving patient care tremendously. Highly precise quantitative surface

deformation information is invaluable when clinicians are striving to achieve natural facial expressions when treating patients with various conditions such as cleft lip and palate and also other clinical settings, such as facial reanimation in the patients with facial paralysis mentioned above. However, there have been technical challenges regarding assessing dynamic motions. Current evaluation of facial expression relies largely on subjective visual evaluation and 2D point to point static distance from 2D static photos, not giving an accurate information about the patients' facial expression patterns, and there has been no studies investigating how to deal with dynamic motions of facial soft tissues [6][7][8] (Figure 2).
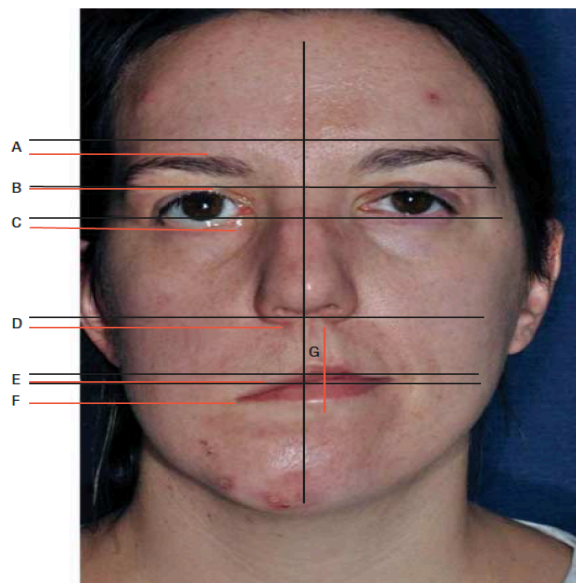

Figure 2: (Adapted from Hadlock et al. [6]) 2D Photograph illustrating 7 relevant distances which were measured in 2D in facial paralysis. Horizontal black lines indicate height of these landmarks on the healthy side, and solid red lines indicate their position on the paralyzed side. The vertical lines represent facial midline based on bisection of the inter-pupillary line in black and the actual center of the philtrum in red.

Advances in medical imaging open nowadays new perspectives for the improvement of the computer assisted surgery planning (CAS), where main goal is to simulate physical interactions with virtual bodies. Realistic simulation of soft issue deformations under the impact of external forces is of crucial importance. In cranio-, dento-maxillofacial surgery, there is a great demand for efficient computer assisted methods, which could enable flexible, accurate, and robust simulations of surgical interventions on virtual patients, including the realistic prediction of their postoperative appearance. Here, soft tissue and facial expressions' modeling have become very critical in creating more realistic virtual patients [9] (Figure 3).
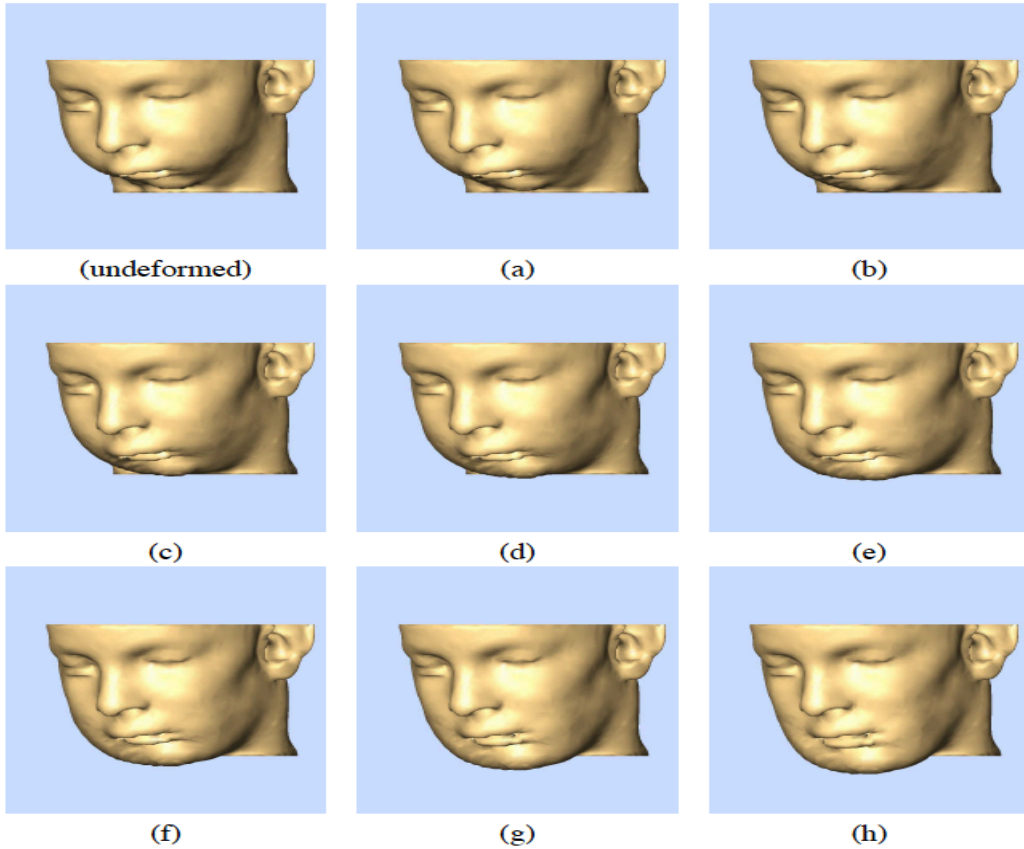
a)

b)
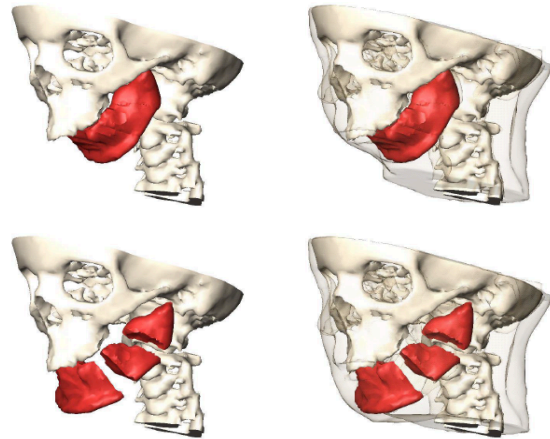
c)

Figure 3: (Adapted from Gladilin. [9]) Soft Tissue Prediction in the CAS Planning (a) A patient with congenital mandibular hypoplasia (b) simulation of mandible distraction (c) resulting soft tissue deformation induced by the stepwise rearrangement of bone structures with maximal boundary displacements of: (a) 0.6 cm, (b) 1.2cm, (c) 1.6cm, (d) 2.0cm, (e) 2.6cm

Orthodontics is a specialty where facial aesthetics has been analyzed with many different ways using Andrew's Goal Anterior-Limit Line (GALL) [10], the ideal smile arc analyzed by Sarver [11], or the Facial Anthropometric Measurements cited by Proffit [12], pursuing improvement in facial aesthetics of patients. However, until recently, two-dimensional imaging

such as cephalometric analysis and 2D static photos have been used in facial analysis [13][14]. However, this conventional 2D method has limitations since 2D methods are utilized to analyze 3D complexities [15] [16].

Three dimensional facial photographic imaging was introduced to orthodontics during the early years of the millennium, allowing visualization of bony anatomy and even more facial soft tissues. Studies have clearly shown that three dimensional imaging modalities have increased accuracy over traditional two-dimensional imaging modalities [18] [19]. To more accurately assess the soft tissues in the paranasal, zygomatic, cheek, and other facial areas, three-dimensional imaging methods such as 3D computerized tomography (CT) and 3D facial scan images (3D-FSI) are needed [17] [20]. However, most current methods in analyzing 3D photographic images rely on subjective visual evaluation or 2D static linear and angular measures between various points to assess facial aesthetics (Figure 4).
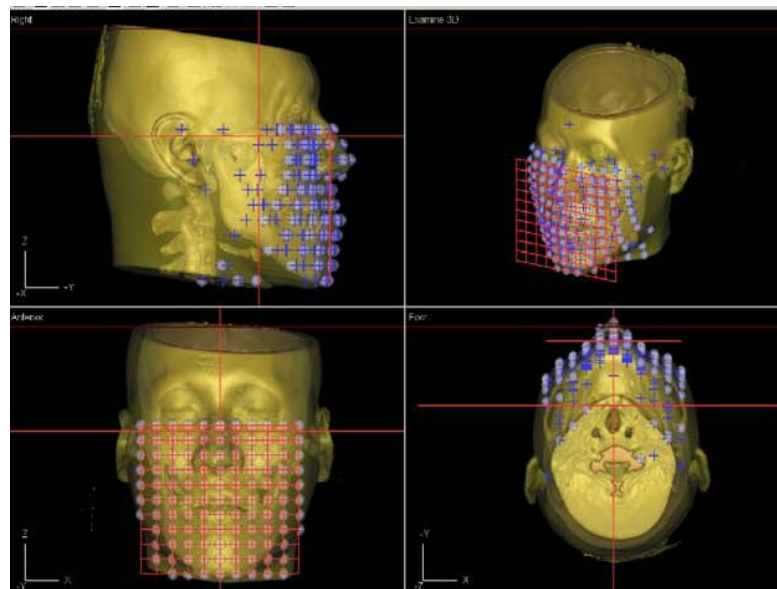

Figure 4: (Adapted from Nam-Kug Kim et al. [21]*) Three-dimensional computed tomography*

grid projected on facial soft tissue demonstrating use of point to point measurements.

Now, with the advances of three dimensional imaging modalities, the orthodontic profession can access to much more information in three dimensions than ever before, and utilizing this valuable information and applying these advancements in imaging towards patient care are necessary. Facial soft tissue analysis has been broadly recognized as a critical factor, leading to successful orthodontic treatment outcomes. However, facial soft tissue is by nature dynamic data, and facial expression is the dynamic movement of these facial soft tissue. Therefore, it is very important to know how to deal with dynamic movement of the facial soft tissue in three dimension, which has never done before.

Up to this point, this invaluable 3dMD data couldn't be utilized due to the lack of the method to analyze dynamic movement of the soft tissues in the 3D facial soft tissue images. Current evaluation of facial expression relies largely on subjective visual evaluation and 2D point to point static distance from 2D static photos, not giving an accurate information about the patients' facial expression patterns [6][7][8]. To our knowledge, there have been no studies investigating in how to quantitatively analyze the dynamic movements of soft tissue in three dimension during facial expressions. Therefore, one of our immediate goal is to use the orthodontic department's 3dMD Imaging System to quantify dynamic movement of facial soft tissues in three dimension.

Ultimately, this research project will contribute to the creation of a dynamic three-dimensional movement trajectory of facial facial expressions and establishment of a new method

to quantitatively track and analyze the changes in soft tissues in 3D while facial expressions are being made. Accomplishing our goal would result in the first new approach for dealing with the dynamic movements of soft tissues in 3D, adding another dimension to the facial analysis in the health care field. Application of this new technology would allow dynamic soft tissue movement (facial expressions) diagnostics for treatment planning in various health care specialties (i.e. orthodontics, oral/maxillofacial and plastic surgery). Once the dynamic facial expression analysis in 3D is completed, this would dramatically change the diagnostic paradigms currently used in craniofacial analysis (2D static facial analysis) towards a totally new and progressive direction (3D facial expression analysis). Potential applications would be 1) generation of normative facial expression patterns across various strata, 2) quantification of treatment effect on facial expression pattern by comparing the average 4D models between T1 and T2, 3) comparison of facial expression patterns between patients with cleft lip/palate and a normative facial expression patterns, and 4) virtual patient creation (currently, we are confined to surface level(shell); by adding muscle mechanics inside soft tissue shell, we can create virtual soft tissue movement and predict those deformations of soft tissue)

Preliminary Studies

This investigation is the first approach in dealing with the dynamic movements of soft tissues in 3D, which will add another dimension to the facial analysis in various health care specialties. There have been no previous studies investigating in dynamic movement analysis.

The most relevant preliminary study relating to this current project was the investigation which further developed the collaboration between the UCLA Section of Orthodontics and the Laboratory of Neurologic Imaging (LONA) at UCLA in order to create a true 3-dimenstional analysis of the human face in 2014: Quantitative Analysis of 3-Dimensional Facial Soft Tissue Photographic Images: Technical Methods and Clinical Application. This project was stimulated by the project funded by the AAOF to map the surface of the human skull in 2012: Craniofacial Surface Mapping: Moving Toward a 3-Dimensional Normative Model of the Human Skull. In the static analysis of facial soft tissue in 2014, certain methodologies from the 2012 craniofacial surface mapping project centered on surface mapping were used as a guideline applicable to the analysis of facial soft tissues [22] (Figure 5).
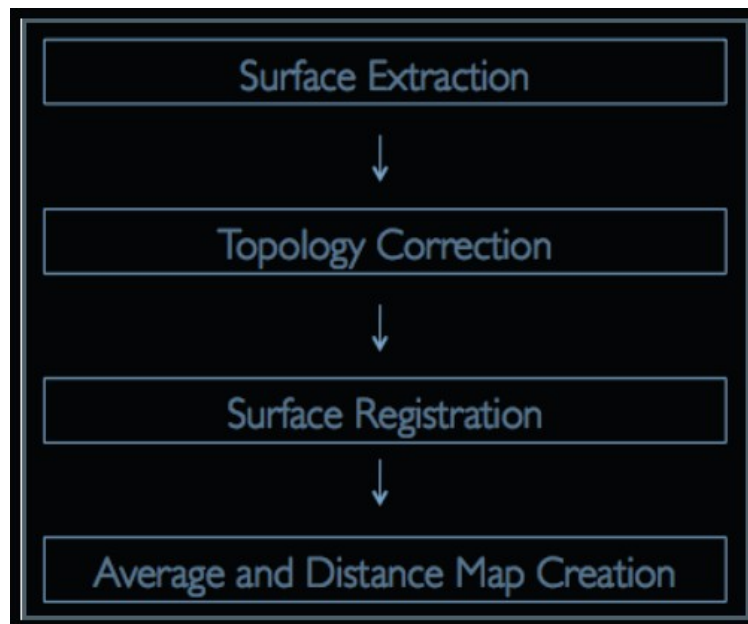

Figure 5: (Adapted from R. McComb. [22]) Diagram illustrating the workflow involved in progressing from a single skull to 3D averages and distance maps

In the previous 2014 study in averaging the human facial soft tissue, static facial soft tissue was averaged, rather than looking at dynamic movements of soft tissues in 3D. The ultimate goal of this project is to develop a new method that has not been investigated before in quantitatively analyzing movement of soft tissues while facial expression is being made, which will open a new door into 3D dynamic facial expression analysis.

Materials and Methods

On a broad level, the project can be divided into five parts, summarized below, and described in more detail in this section:

1. Development of dynamic system (via. mathematical modeling)
2. Data Collection
    a. 3dMD Imaging Protocol
    b. Facial Expression Taking Protocol
    c. Collection of 3D face models at five different time points (T_1, T_2, T_3, T_4, T_5) while facial expression is being made
3. Data Processing
    a. Classification of smiling patterns / Generation of homogenous samples
    b. Vertex correspondence of 3D meshes
    c. Landmarking
4. Average and creation of displacement vectors in MATLAB
    a. Average samples at five different time points

b. Computation of displacement vectors between each time point

5. Statistical Analysis in MATLAB & Dynamic Visualization

a. Computation of p values in 3 dimension at all landmarks

b. Creation of color-coded displacement vector p maps between each time point
with p values in 3D

c. Dynamic visualization of averaged smiling movement trajectory

I. Development of Dynamic System (via. mathematical modeling)

The main purpose of this project is to develop a method that quantifies the dynamic movements of soft tissue in three dimension while smiling is made. Facial soft tissue can be thought of as a whole entity comprised of infinite numbers of points on the epidermis, that is, superficial points on the facial surface, which is by nature dynamic, which moves over time. During facial expressions, those points on the facial surface move but at the different rate [9][23] (Figure 6).
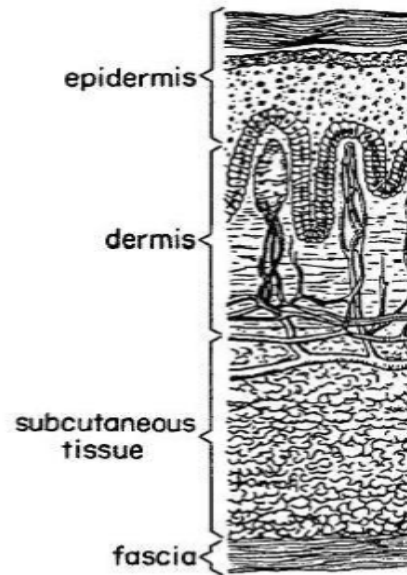
Figure 6: (Adapted from Gladilin [9]) A typical cross-section of facial tissue

Then, how can we describe dynamic movement of moving objects in mathematical functions? Objects can be largely classified into two kinds: 1) inanimate object 2) deformable object (facial soft tissue). In inanimate objects, all the points move equal amount. However, in deformable objects which were my interest in this research project (facial soft tissue), all the points are not moving at the same rate or amount [23]. Most points which move during facial expression are usually those points around eyes, nose, and lips. Therefore, it makes sense to look at landmarks, which are easy to recognize. In this research project, landmarks will be quantitatively tracked.

If objects move from one point in one plane to the other point in another plane, then it can be described by the mathematical function phi [9] (Figure 7).
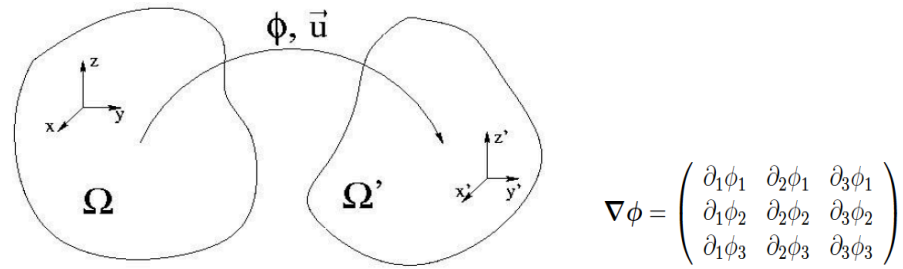
$$\nabla \phi = \begin{pmatrix} \partial_1\phi_1 & \partial_2\phi_1 & \partial_3\phi_1 \\ \partial_1\phi_2 & \partial_2\phi_2 & \partial_3\phi_2 \\ \partial_1\phi_3 & \partial_2\phi_3 & \partial_3\phi_3 \end{pmatrix}$$

Figure 7: (Adapted from Gladilin [9]) 3D domain deformation (here, the deformation gradient

$\nabla\emptyset$ in matrix)

Moving objects can be described as either 1) trajectories and/or 2) equations of motions. Modern tracking technology like GPS, cell phone, and even sensor networks are being heavily used, and spatio-temporal data generated by mobile devices (trajectories of moving objects) provide characteristic of space and time. There have been researches trying to discover chasing behavior in moving object trajectories. This can help analyze where something happened and when it happened. These trajectory data can express different behaviors through space and time such as move faster, change direction, stand still, and repeat the same route, and this concept of trajectory can be applied in my research project [24][25][26][27] (Figure 8) .
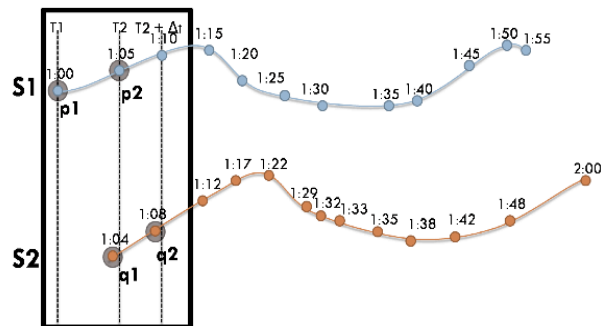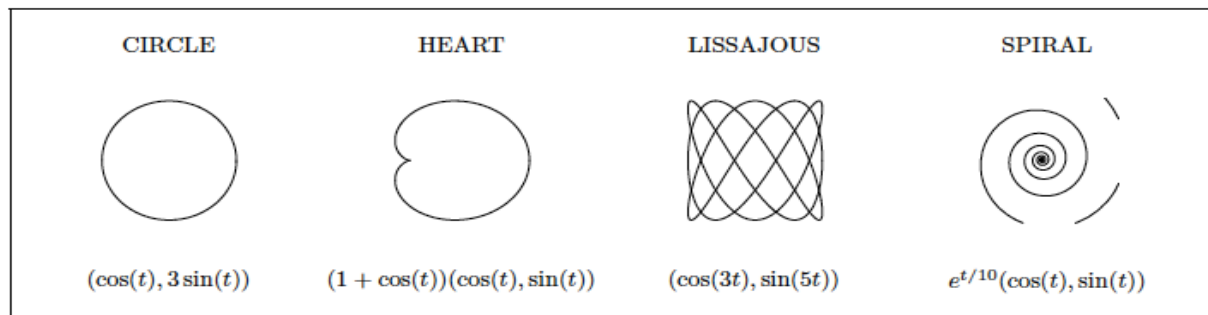
Together with the trajectory, mathematical equations of motions to describe movements are to be used. In physics and mathematics, equations of motions have been used to describe moving objects. Let $x(t) = (x_1(t), \ldots, x_n(t))$ denote the location of a point particle in R^n at time t. The velocity of the particle at time t is given by $v(t) = \dot{x}(t) = \frac{d}{dt}x(t)$. By Newton's Second Law, the motion is fully described once we know the force $F(t)$ acting on the particle. The motion is described by the unique solution of the differential equation of motion shown below.

$$F(t) = m\frac{d^2}{dt^2}x(t), \quad x(t_0) = x_0, v(t_0) = v_0$$

in which m denotes the mass of particle and $x(t_0) = x_0$ and $v(t_0) = v_0$ are initial conditions [24][30][31]. In this study, $F(t)$ is the force from underlying muscles and m is the mass of those landmarks, which can be assumed as massless point particles.

There are also different mathematical equations which can describe different types of motions of moving objects (Figure 9).
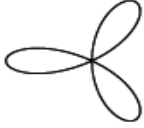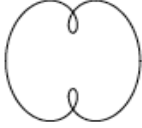

CIRCLE	HEART	LISSAJOUS	SPIRAL
$(\cos(t), 3\sin(t))$	$(1 + \cos(t))(\cos(t), \sin(t))$	$(\cos(3t), \sin(5t))$	$e^{t/10}(\cos(t), \sin(t))$

TRIFOLIUM	EPICYCLE	SPRING (3D)	TORAL KNOT (3D)
$-\cos(3t)(\cos(t), \sin(t))$	$(\cos(t) + \cos(3t)/2, \sin(t) + \sin(3t)/2)$	$(\cos(t), \sin(t), t)$	$(\cos(t) + \cos(9t)/2, \sin(t) + \cos(9t)/2, \sin(9t)/2)$

Figure 9: Different mathematical equations to describe different types of movement trajectories

of moving objects $(r(x, y, z, t), r(r, \theta, z, t), r(r, \phi, \theta, t))$

Let's go back to the physics of motion again [24][30][31][32][33]. Again, the motion is described by the unique solution of the differential equation of motion

$$\boldsymbol{F}(t) = m \frac{d^2}{dt^2} \boldsymbol{x}(t), \quad \boldsymbol{x}(t_0) = \boldsymbol{x_0}, \boldsymbol{v}(t_0) = \boldsymbol{v_0}$$

(here, m denotes the mass of particle, $\boldsymbol{x}(\boldsymbol{t_0}) = \boldsymbol{x_0}$ and $\boldsymbol{v}(\boldsymbol{t_0}) = \boldsymbol{v_0}$ are initial conditions)

Higher-order differential equations can always be transformed into first-order ones by adding variables. Therefore, the second-order equation above is equivalent to the first-order equation shown below.

$$\frac{d}{dt} \boldsymbol{X}(t) = \frac{d}{dt} \begin{pmatrix} \boldsymbol{x}(t) \\ \boldsymbol{v}(t) \end{pmatrix} = \begin{pmatrix} \boldsymbol{v}(t) \\ \boldsymbol{F}(t)/m \end{pmatrix}$$

Solution for the equations above describe the motion of moving objects. Some equations can be solved analytically. However, this is not always the case, and often needs to rely on numerical integration techniques to obtain some information about the solution [32]. Commonly used methods include Euler's method and higher-order (adaptive) Runge-Kutta methods.

Since $F(t)$ (force from muscle) is unknown and point objects (landmarks) are massless, another approach needs to be used and in my research what is known as physically based modeling in computer graphics is used.

In physically based modeling [29],

$$\dot{x} = f(x, t)$$

where, f is known function (i.e. something we can evaluate given x and t), x is the state of the system, and $\dot{x}$ is x's time derivative. Typically, x and $\dot{x}$ are vectors. This ordinary differential equation (ODE) shown above is the principal equation, describing the behavior of the dynamic system. In an initial value problem (IVP), we are given $x(t_0) = x_0$ at some starting time t_0, and wish to follow x over time thereafter. If we are given initial point, then we can follow x overtime thereafter by using the main equation. Here, we could get rid of mass and force which are unknown in our situation.

Derivative function f defines a vector field on the plane (Figure 10(a)) and the vector at x is the velocity that the moving point must have if it ever moves through x. Thinking of f as driving force from point to point, like an ocean current. Wherever we initially deposit **p**, the "current" at that point will seize it. Where **p** is carried depends on where we initially drop it, but once dropped, all future motion is determined by f. The trajectory swept out by **p** through f forms an *integral curve* of the vector field [29] (Figure 10(b)).

(a)   (b)

The derivative
function

$\dot{x} = f(x,t)$
forms a vector
field.

Start Here

Follow the vectors…

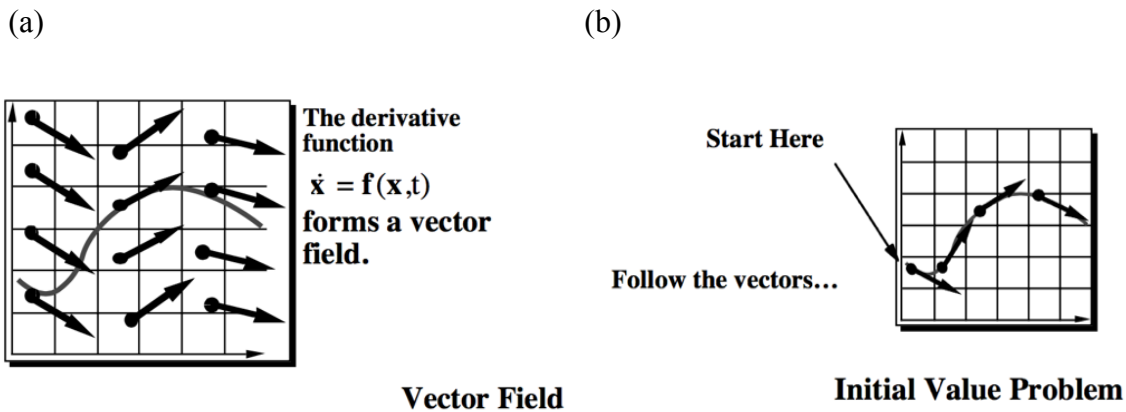**Vector Field**   **Initial Value Problem**

Figure 10: (Adapted from Andrew Witkin and David Baraff [29]) (a) The derivative function

f(x,t). defines a vector field (b) An initial value problem. Starting from a point x_0, move with

the velocity specified by the vector field

As far as solutions to this derivative function, there can be two different kinds of solutions:

1) symbolic solution 2) numerical solutions. Standard introductory differential equation focuses

on symbolic solutions, where the functional form for the unknown function is to be guessed.

However, in numerical solution method, discrete time steps starting with the initial value $x(t_0)$

are taken, and the derivative function $f(x, t)$ is used to calculate an approximate change in x (Δx)

over a time interval Δt, and new value is obtained by incrementing x by Δx.

There are different methods to find the solution for the ODE such as Euler's method,

Taylor Series, Midpoint method, and Runge-Kutta method. Among different methods, Euler's

method is the simplest even though it could be less accurate. At the beginning the vector f is

evaluated and then scaled by Δt (*or* h) (time duration or a stepsize parameter). Let our initial

value for x be denoted by $x(t_0) = x_0$ and our estimate of x at a later time $t_0 + h$ by $x(t_0 + h)$, where h is a stepsize parameter. Euler's method simply computes $x(t_0 + h)$ by taking a step in the derivative direction.

In Euler's method, instead of the real integral curve, **p** follows a polygonal path, each leg of which is determined by evaluating the vector **f** at the beginning, and scaling by **h** (Figure 11(a)) [29]. There are several problems in this method. Bigger time duration results in bigger errors. Consider the case of a function whose integral curves are concentric circles. A point **p** governed by **f** is supposed to orbit forever on whichever circle it started on. Instead, with each Euler step, **p** will move on a straight line to a circle of larger radius, so that its path will follow an outward spiral. Shrinking the stepsize will slow the rate of this outward drift, but never eliminate it (Figure 11(b)). Instability is another problem of this method. It is known that too large step-size could make the system unstable [29].
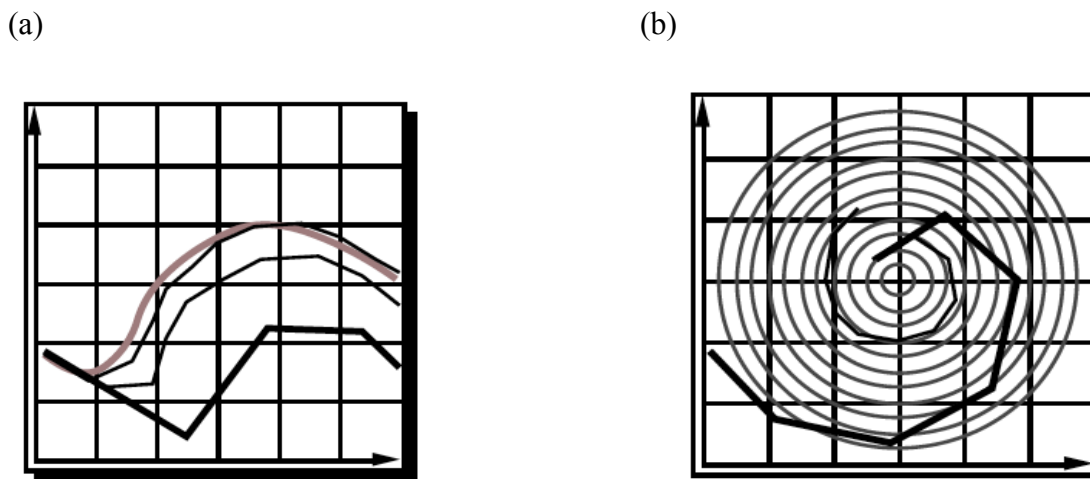
(a)   (b)

Figure 11: (Adapted from Andrew Witkin and David Baraff [29]) (a) An initial value problem. Starting from a point x_0, move with the velocity specified by the vector field (b) Inaccuracy: Error turns x(t) from a circle into the spiral of your choice.

23

To improve on Euler's method, Taylor series including higher-order derivatives can be used. Taylor series:

$$\mathbf{x}(t_0 + h) = \mathbf{x}(t_0) + h\dot{\mathbf{x}}(t_0) + \frac{h^2}{2!}\ddot{\mathbf{x}}(t_0) + \frac{h^{3\dots}}{3!}\mathbf{x}(t_0) + \dots + \frac{h^n}{n!}\frac{\partial^n \mathbf{x}}{\partial t^n} + \dots$$

Assuming $x(t)$ is smooth, we can express its value at the end of the step as an infinite sum involving the value and derivatives at the beginning. As can be seen above, we get the Euler update formula by *truncating* the series, discarding all but the first two terms on the right hand side. This means that Euler's method would be correct only if all derivatives beyond the first were zero, i.e. if $x(t)$ were linear. The *error term,* the difference between the Euler step and the full, un-truncated Taylor series, is dominated by the leading term, $(h^2/2)\ddot{x}(t_0)$. Consequently, we can describe the error as $O(h^2)$ (read "*Order h squared*"). If the derivative function is linear, then Euler's method can provide quite accurate solution with simplicity.

In midpoint method, we truncates all but the first three terms, that is, one additional term will stay, resulting in less error compared to Euler's method. That is, if we were able to evaluate $\ddot{x}$ as well as $\dot{x}$, we could achieve $O(h^3)$ accuracy instead of $O(h^2)$ simply retaining one additional term in the truncated Taylor series:

$$\mathbf{x}(t_0 + h) = \mathbf{x}(t_0) + h\dot{\mathbf{x}}(t_0) + \frac{h^2}{2}\ddot{\mathbf{x}}(t_0) + O(h^3).$$

We don't have to stop with an error of $O(h^3)$. By evaluating f a few more times, we can eliminate higher and higher orders of derivatives. The most popular procedure for doing this is a method called Runge-Kutta of order 4 and has an error per step of $O(h^5)$. The Midpoint method could be called Runge-Kutta of order 2. We won't derive the fourth order Runge-Kutta method,

but the formula for computing $x(t_0 + h)$ is listed below:

$$
\begin{aligned}
k_1 &= hf(\mathbf{x}_0, t_0) \\
k_2 &= hf(\mathbf{x}_0 + \frac{k_1}{2}, t_0 + \frac{h}{2}) \\
k_3 &= hf(\mathbf{x}_0 + \frac{k_2}{2}, t_0 + \frac{h}{2}) \\
k_4 &= hf(\mathbf{x}_0 + k_3, t_0 + h) \\
\mathbf{x}(t_0 + h) &= \mathbf{x}_0 + \frac{1}{6}k_1 + \frac{1}{3}k_2 + \frac{1}{3}k_3 + \frac{1}{6}k_4.
\end{aligned}
$$

In addition, time duration or step-size h (which could be fixed or adaptive) in every method has an impact on the outcome. Whenever we can make h large without incurring too much error, we should change time duration. When h has to be reduced to avoid excessive error, we want to adapt time duration as well. This is the idea of adaptive stepsizing: varying h over the course of solving the ODE [29].

Based on the pros and cons of the methods, Euler's method was applied in our project. Derivative function $\dot{x} = f(x, t) = \frac{x(t+\Delta t) - x(t)}{\Delta t}$ is the function we are interested in this project. Since step size $\Delta t \approx h$ is pre-determined, displacement vector between each time point will be computed in our project.

The trajectory of a moving point can be modeled by a function of time, represented by the real line $\mathbb{R}$, to the n-dimensional space $\mathbb{R}^n$. A function from $\mathbb{R}$ to $\mathbb{R}^n$ is linear if it has the form $x = at + b$ where a, b are vectors in $\mathbb{R}^n$; A function is *piecewise linear* if it consists of a finite number of linear pieces, i.e., if it has the form

$$
x = \begin{cases}
a_1 t + b_1 & \text{if } t_0^{(1)} \leq t \leq t_1^{(1)} \\
\quad \vdots & \qquad \vdots \\
a_k t + b_k & \text{if } t_0^{(k)} \leq t \leq t_1^{(k)},
\end{cases}
$$

25

where $t_1{}^{(i)} \leq t_0{}^{(i+1)}$ for all $i = 1, ..., k$ [29].

II.   Data Collection

1. 3dMD Imaging Protocol

Soft tissue is by nature dynamic and changes significantly depending on acquisition methods,

yielding a range of data. Therefore, formulating a method of standardizing image acquisition is

important. The following is the protocol which can obtain consistent 3D photographic images.

a.   3dMD Room Setup

A rectangular room with dimensions of 2.09m x 2.94m at the department of Orthodontics was

used for our 3dMD system. A virtual 1:1 scale model based on actual measurements was

generated of the room and equipment which represent an accurate ratio. To visualize the set up

necessary for the 3dMD system, a 3D animation and modeling software called Houdini^{TM} by

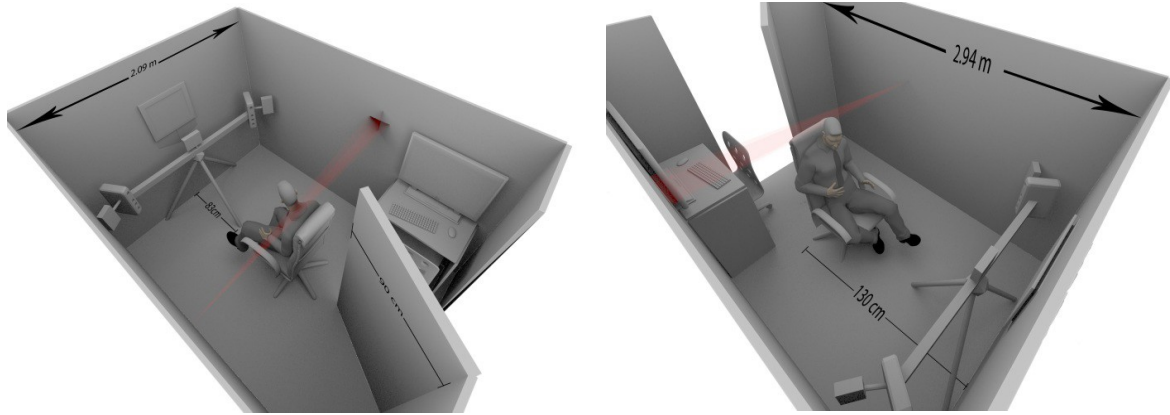Side Effects Software Incorporated was used (Figure 12).

Figure 12: Custom modeled set-up for UCLA Orthodontic Department 3dMD System

b. Natural Head Posture (NHP)

Since Natural head posture (NHP) has been shown to be clinically reproducible, NHP was adopted for this study [34] [35] [36]. Having subjects sitting on the adjustable chair, they were instructed to look into a mirror at front with horizontal and vertical lines marked. They were instructed to level their eyes to the horizontal line and align the midline of their face with the vertical line. The seating height was also adjusted to achieve natural head posture if necessary. Right before the 3dMD images were taken, subjects were instructed to swallow hard and to keep their jaws relaxed. Each image acquisition time duration was 1.5 ms [37]. To measure the reliability of a particular imaging system, a previous study published in the AJO-DO used a laser system at different time points, and (*Figure 13*) shows the positioning we pursue to achieve consistent NPH throughout our study [38].
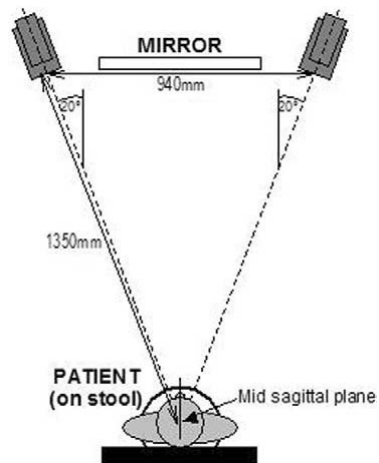
Figure 13: (Adapted from H. K. Chung [38]*) Reproducible patient positioning method for*

Natural Head Position

c. System Calibration

In order to maintain consistent orientation and positioning across time points, a calibration plate

and tripod were used each morning before daily image acquisitions for calibrating the camera

system /software in images in our investigations.

2. **Facial Expression Taking Protocol**

Since this study is developing the protocol to quantity dynamic movement of soft tissues in 3D

for the first time, cleanness and homogeneity of samples are critical to validate the novel

methodology. Therefore, facial expressions templates (Figure 15, Figure 16) were provided

before they came to take facial expressions and asked them to practice to generate homogenous

facial expressions [42][43][44].

On the day of taking 3dMDs, templates of facial expressions were provided to remind them. 3dMDs were taken when participants were ready, asking them to make facial expression very slowly. 3dMD photos were taken from starting of facial expression till the end at five different time points, i.e., T_1, T_2, T_3, T_4, T_5 while facial expression was being made. The following is how the time points should be captured [39][40][41]. (Figure 14) is an example of 3D dynamic data sequence.

T1: Neutral/Resting

T2: Mid-way through smile/frown/etc.

T3: Complete smile/frown/etc.

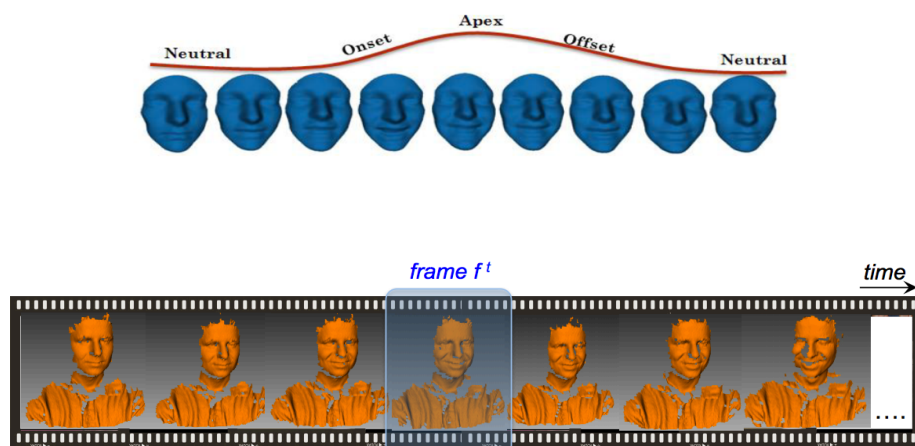**T4: Mid-way back to resting position**

T5: Neutral/Resting

Figure 14: (Adapted from Taleb Alashkar et al. [39]) Equally-spaced 3D frames of a sample dynamic facial sequence conveying a happiness expression.

29

Even though smiling patterns will be our main interest in our project, seven different facial expressions were recorded 1) smile, 2) surprise, 3) sadness, 4) anger, 5) fear, 6) disgust, 7) contempt for future use once this dynamic system is developed.
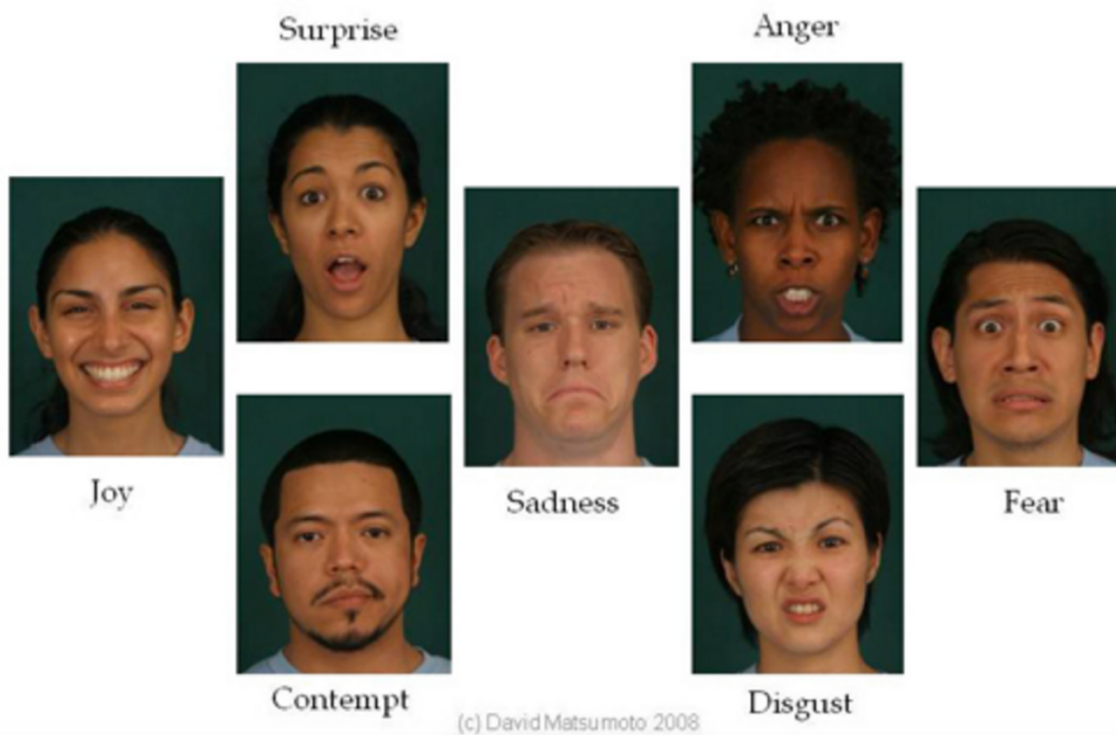

Figure 15: Templates of facial expressions which were given to the participants of this study/

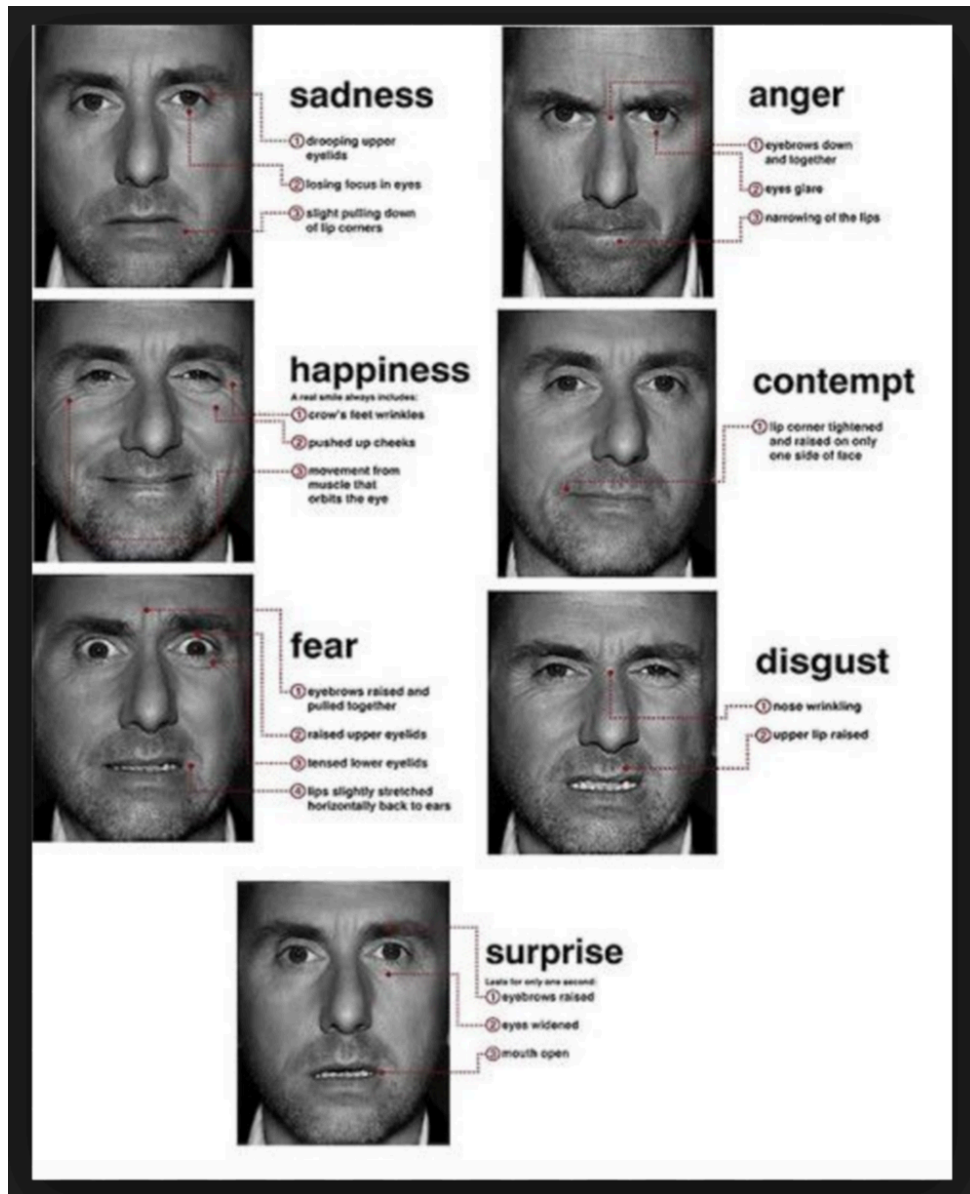*The Seven Universal Facial Expressions of Emotion [44]*

Figure 16: Templates of facial expressions which were given to the participants of this study/ Basic assumptions of Ekman's facial action coding system illustrated using the face of Tim Roth, the actor portraying Dr. Cal Lightman in Lie to Me – a tv drama employing FACS to solving crimes [42][43][45]

3. **Collection of 3D face models at five different time points while facial expression is being made**

A standard protocol for consistent image acquisition in using the 3dMD system is required. The protocol which was used in Dr. Nanda's study [59] was used in our study to obtain consistent 3dMD images of individual subjects while facial expression is being made. 3dMD system (3dMD, Atlanta, Ga) is known as a structured light system which combines stereo- photogrammetry and the structured light technique. This system uses a multi- camera configuration where three cameras (one color camera, two infrared cameras) are used to capture photorealistic face models. 3dMD facial images which contain from ears to under the chin can be obtained in 1.5 ms with the highest resolution. Participants were recruited and 3dMDs of the participants were collected following facial expression taking protocol above. The following is one demonstration of five frontal views of 3dMDs taken from 3dMD Imaging System at five different time points (Figure 17).

Figure 17: Demonstration of five frontal views taken from 3dMD Imaging System at five different time points (from left, T_1, T_2, T_3, T_4, T_5)

III. Data Processing

1. Classification of smiling patterns (4 groups) / Generation of homogenous samples based on inclusion criteria

3dMDs of participants while smiling was studied, and the classification criteria was set based on those. Smiling expressions of all participants were classified into four different groups based on the curvature of upper lip's inner line (group1: negative curvature, group 2: zero curvature & flat, group 3: positive curvature, and group 4: lips closed) (Figure 19). For reference, curvature is defined as a two-dimensional property of a curve and describes how bent a curve is at a particular point on the curve i.e. how much the curve deviates from a straight line at this point [46] (Figure 18).
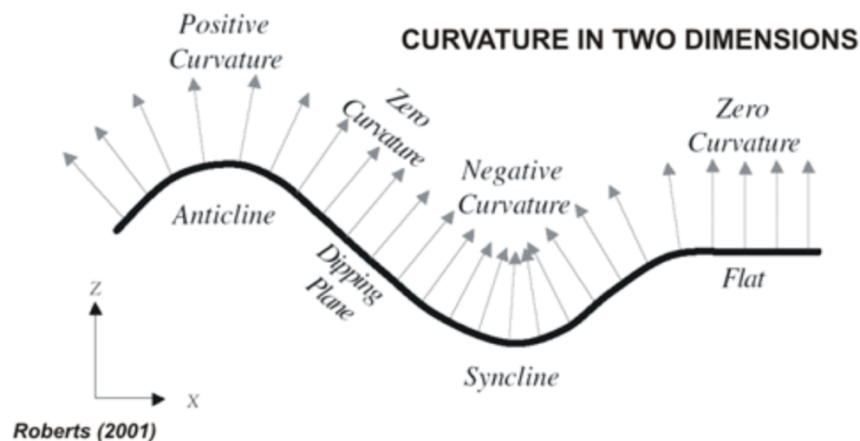

Figure 18: Sign convention for curvature attributes. The grey arrows represent vectors, which are normal to the surface. Where these vectors are parallel on flat or planar dipping surfaces, the curvature is zero. Where the vectors diverge over anticlines, the curvature is defined as positive and where they converge over synclines, the curvature is defined as negative.
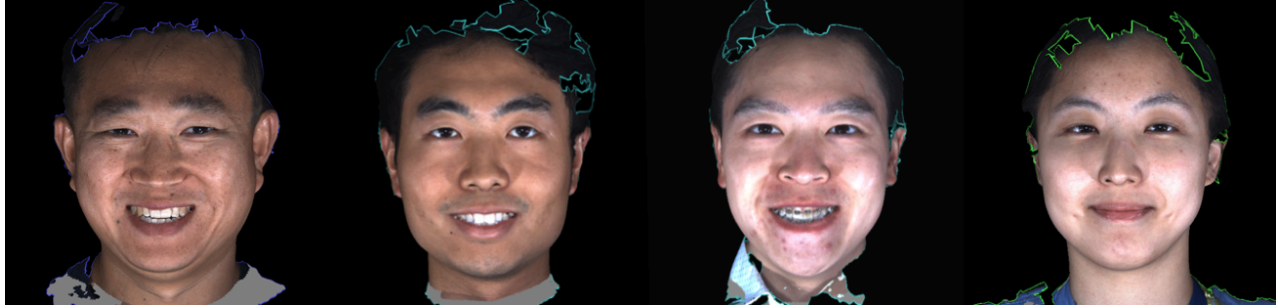
33

Figure 19: Examples of classified smiling patterns. From left, 3dMD frontal views of group 1, group2, group3, and group 4 smiling patterns

2. Vertex correspondence of 3D meshes

Establishing vertex correspondence between 3D meshes is important in studying dynamic movement of facial soft tissues. By establishing correspondence between vertices in one mesh and vertices in the other mesh, we can track the vertex motion. This has been quite challenging [47][48][49][50]. Registration refers to the alignment of two or more surfaces so that they overlay each other in 3D space. There are many methods such as surface-based registration (whole surfaces or selected regions) and registration via manually selected points. In my project, this was established through 3dMD surface registration (whole surfaces) method and minimizing root mean square (RMS) errors, which were obtained between each time point and between each individual.

3. Landmarking

As mentioned above, in deformable objects (facial soft tissues), all the points are not moving at the same rate or amount [9][23]. Most points which move during facial expressions are usually points around eyes, nose, and lips. Therefore, it makes sense to look at landmarks, which are easy to

recognize. These landmarks can be applied to triangular mesh later. In this research project, 28 landmarks were quantitatively tracked, and these were chosen in 4 major sub-regions where most of movements occur while facial expressions are being made (Oral region: 10 landmarks, Nasal region: 4 landmarks, Eye region: 8 landmarks, and Eyebrow region: 6 landmarks). These sub-regions were chosen based on the responsible major muscle groups in face. Dr. Ekman and Dr. Friesen developed Facial Action Coding Systems (FACS) in 1978 based on facial muscle change to characterize facial actions which constitute a facial expression. FACS encodes the movement of specific facial muscles called Action Units (AUs), which reflect distinct momentary changes in facial appearance [53][54][55][56] (Figure 20). Landmarking refers to placing landmarks on a subject. Landmarking was performed for all the included 3dMD data, generating landmarking files which were imported into MATLAB for data analysis. The landmarks used were shown below (Figure 21, Table 1,2,3,4).
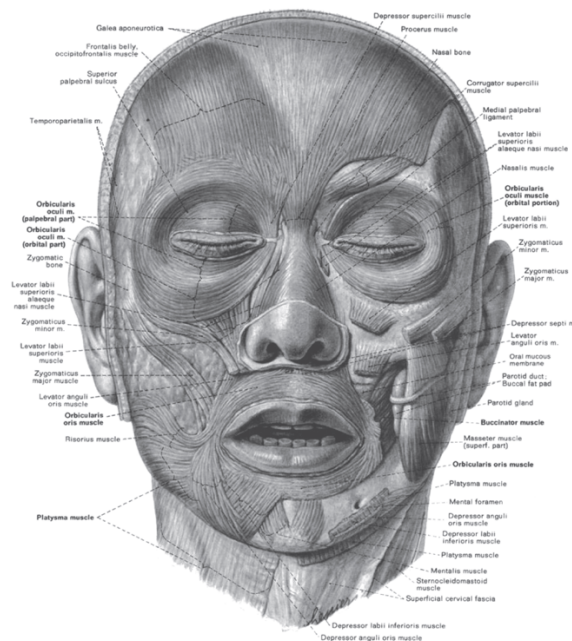

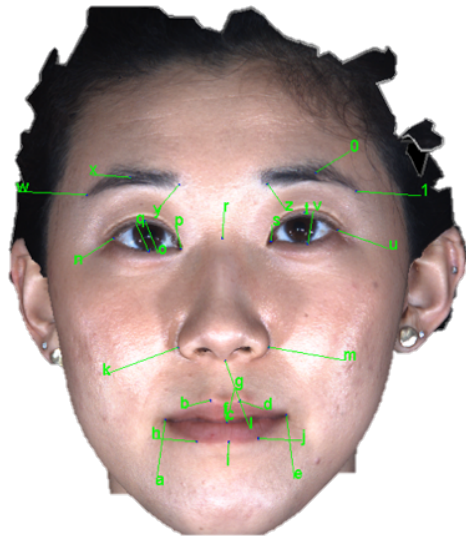*Figure 20: (Adapted from Clemente [58]) Muscles of the face which contribute facial*

expressions
35

Figure 21: Illustration of one participant 3dMD face model at T1(frontal view) showing all 28 landmarks used in this project placed.

Landmarks in 3dMD	Landmarks # in MATLAB	
a	1	Right mouth corner
b	2	Right upper lip
c	3	Upper lip center
d	4	Left upper lip
e	5	Left mouth corner
f	6	Inner upper lip
g	7	Inner lower lip
h	8	Right lower lip

i	9	Lower lip center
j	10	Left lower lip

Table 1: 10 Landmarks used around the mouth (oral region)

Landmarks in 3dMD	Landmarks # in MATLAB	
k	11	Right alar base
l	12	Sub-nasale
m	13	Left alar base
r	18	Glabella

Table 2: 4 Landmarks used around the nose (nasal region)

Landmarks in 3dMD	Landmarks # in MATLAB	
n	14	Right outer eye corner
o	15	Right upper eye center
p	16	Right inner eye corner
q	17	Right lower eye center
s	19	Left inner eye corner
t	20	Left upper eye center
u	21	Left outer eye corner
v	22	Left lower eye center

Landmarks in 3dMD	Landmarks # in MATLAB	
w	23	Right outer eyebrow
x	24	Right eyebrow center
y	25	Right inner eyebrow
z	26	Left inner eyebrow
0	27	Left eyebrow center
1	28	Left outer eyebrow

Table 4: 6 Landmarks used around the eyebrows (eyebrow region)

IV.   Average and creation of displacement vectors in MATLAB

1.   Average samples at five different time points

To compute the average smiling face model at each different time point, once landmarking process was complete, those 3dMD files were imported into MATLAB for quantification. Vector representation of all landmarks were done and averaging functions were programmed along with statistical functions to produce standard deviations and ranges in MATLAB. Each landmark has corresponding x,y,z coordinate on a Cartesian coordinate. Each averaged landmark has not only mean values of those x, y, z coordinates but also has a specific standard variation, representing statistical point.

2. **Computation of displacement vectors between each time point**

Having computed the average smiling face models at each time point T1, T2, T3, T4, and T5, the displacement vectors between each time point, i.e., between T1 and T2, T2 and T3, T3 and T4, T4 and T5 were computed in MATLAB, producing the average displacement vectors for smiling movement. In the displacement vector maps, each averaged point will have directional vectors where the length of the vector can represent the magnitude of displacement, arrow of the vector shows the direction of the displacement, and the color of the vector will indicate the significance level of the movement of the landmark.

V. **Statistical Analysis in MATLAB & Dynamic Visualization**

1. **Computation of p values at all landmarks in 3 dimension**

Since each averaged landmark at each time point is a statistical point which has a mean, standard deviation, and statistical p value, not only displacement vectors but also statistical p values of all landmarks need to be computed to see if which landmarks and when those landmarks have shown significant level of displacement during smiling movement. Previously, p values were computed in each x, y, z axis separately. However, this method could not give accurate information since even though displacement along each axis does not show significant movement, total displacement in 3 dimension could show significant movement [59]. For more accurate computations of p values in three dimensions, a new approach was developed by switching the coordinate system from the Cartesian coordinate to Spherical coordinate where distributive radii of all landmarks at each

different time point were used as random variables. Based on this new approach, p values in three dimensions of all landmarks between each time point were computed via. paired sample t-test at the 5% significance level ($\alpha = 0.05$).

2. **Creation of color-coded displacement vector maps between each time point with p values in 3D of all landmarks**

P values of all landmarks were classified into three different groups and color-coded based on the significance level ($\alpha = 0.05$) between each time point: severely significant ($p < 0.01$, red), significant ($0.05 < p < 0.01$, yellow), and insignificant ($p > 0.05$, blue). Then, color-coded displacement vector maps (p maps) between each time point were generated.

3. **Dynamic visualization of averaged smiling movement representation**

For visualization of the averaged smiling movement from T1 through T5 while smiling is being made, average landmarks at each different time point were tracked and trajectories were visualized dynamically by creating a continuous animation of the average smiling motion representation over time from T1 through T5.

Results

A. **Data Collection**

In total, 29 Participants were recruited at the UCLA Orthodontics Clinic. 3dMDs of all 29 participants were taken from starting of facial expression till the end at five different time points, i.e., T_1, T_2, T_3, T_4, T_5 while smiling was being made (T1: Neutral/Resting, T2: Mid-way through smile/frown/etc., T3: Complete smile/frown/etc., T4: Mid-way back to resting position, T5: Neutral/Resting). Even though smiling patterns were our main interest in our project, seven different facial expressions were recorded 1) smile, 2) surprise, 3) sadness, 4) anger, 5) fear, 6) disgust, 7) contempt for future use.

The following table shows the demographics of the 29 participants.

Total sample number n = 29	
Gender	Female(16) Male(13)
Ethnicity	Korean(18), Chinese(7), Indian(1), Hispanic(1), Persian(1) Caucasian(1)
	Korean (18): Female(8), Male(10)
	Chinese (7): Female(5), Male(2)
	Others (4): Female(3), Male(1)
Age	23 yrs 9 months ~ 43 yrs 2 months

Table 5: Demographics of the initial 29 participants for our study

B. Data Processing

3dMD face models of all participants while smiling was classified into four different groups based on the curvature of upper lip's inner line (group1: negative curvature, group 2: zero

41

curvature & flat, group 3: positive curvature, and group 4: lips closed) (Figure 22). 18 participants were in group 1, 9 participants were in group 2, 1 participant in group 3, and 1 participant in group 4. Since most of the participants were in group 1, group 1 was initially included for data analysis. Vertex correspondence between 3d meshes between individual and time point was performed via surface-based registration method and minimizing root mean square (RMS) errors, which were obtained between each time point and between each participant. Based on the RMS errors, 10 participants were finally included in our analysis (Figure 23).
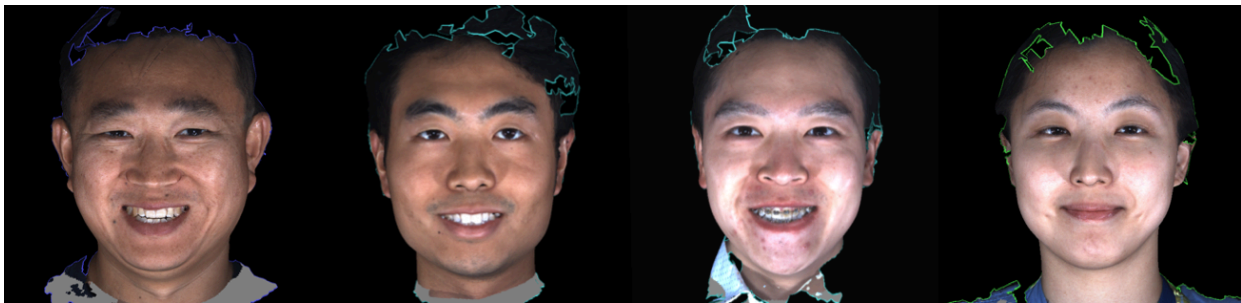
Figure 22: Examples of classified smiling patterns. From left, 3dMD frontal views of group 1, group2, group3, and group 4 smiling patterns (Repeat of Figure 19 - Here for visual purposes).

Figure 23: 10 individual 3dMD samples finally included in our analysis to create average smiling movement representation at five different time points, i.e., T_1, T_2, T_3, T_4, T_5 from starting of facial expression till the end while smiling is being made. From left, T_1, T_2, T_3, T_4, T_5 (Only frontal views are shown in this figure)

Since all the points on the face do not move at the same rate or amount while facial expression is being made and it is known that most points which move during facial expression are usually points around eyes, nose, and lips, 28 recognizable landmarks were determined to be used in our project (Oral region: 10 landmarks, Nasal region: 4 landmarks, Eye region: 8 landmarks, and Eyebrow region: 6 landmarks) (Figure 24). Landmarking was performed for the finally included samples, generating landmarking files which were imported into MATLAB for data analysis.
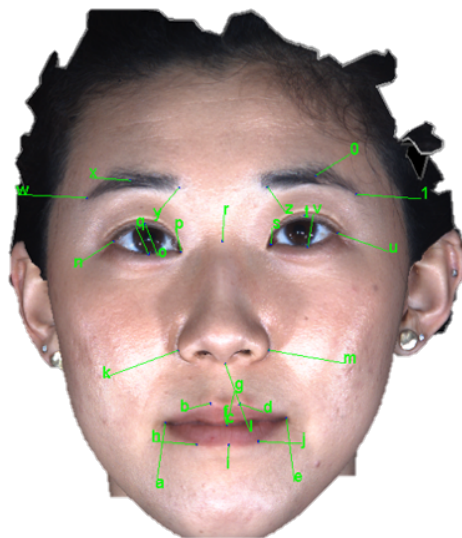
Figure 24: Illustration of one participant 3dMD face model at T1 (frontal view) showing all 28 landmarks used in this project placed (Repeat of Figure 21 - Here for visual purposes).

C. 3D facial landmark average at five different time point (T1, T2, T3, T4, and T5) while smiling is being made

The finally included 10 participants' 3dMD facial models at 5 different time points were loaded into the MATLAB after being in vertex correspondence and landmarking process for quantification. Vector representations of all landmarks were conducted, and averaging functions were programmed along with statistical functions in MATLAB. The average landmarks of 10

participants at five different time point from the beginning of the smiling till the end were generated. The following shows the averaged landmarks at each different time point while smiling was being made (Figure 25, 26, 27, 28, 29). Here, each point is the statistical point with the mean, standard deviation, and the range.
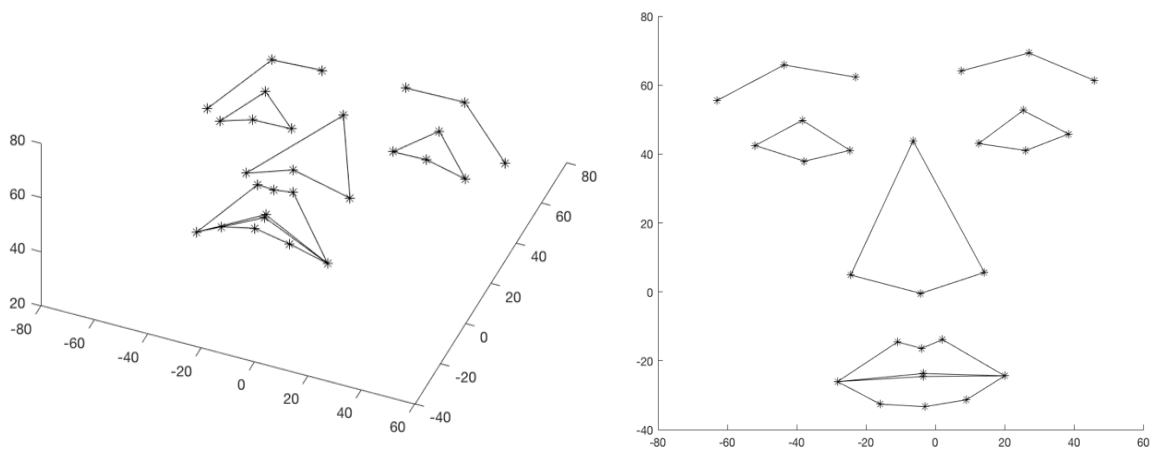

Figure 25: landmark average of 10 individual samples at time point T1 while smiling movement was being made: "The Average smiling face model at T1"
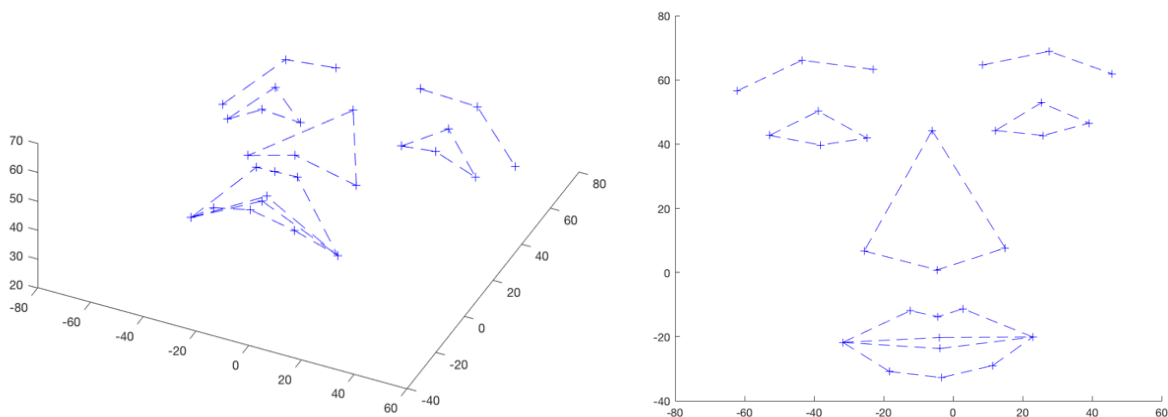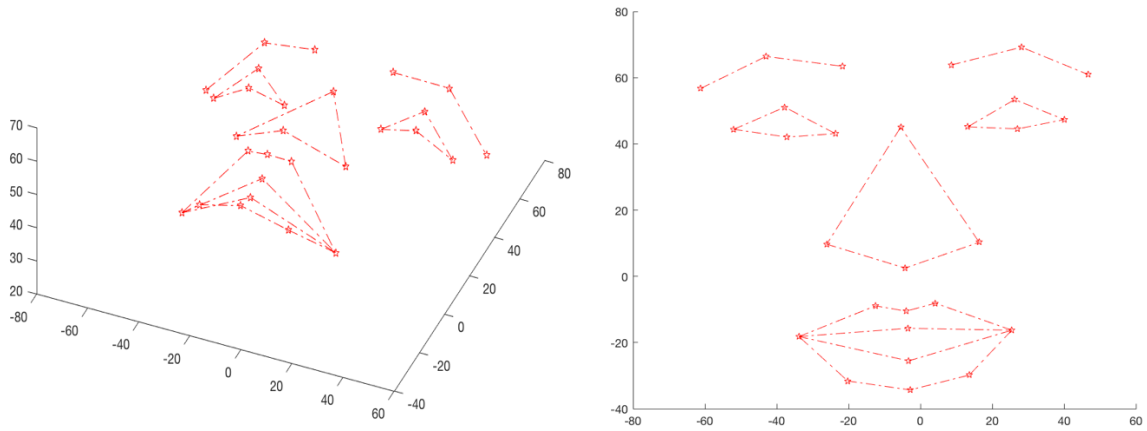
Figure 27: landmark average of 10 individual samples at time point T3 while smiling movement was being made: "The Average smiling face model at T3"
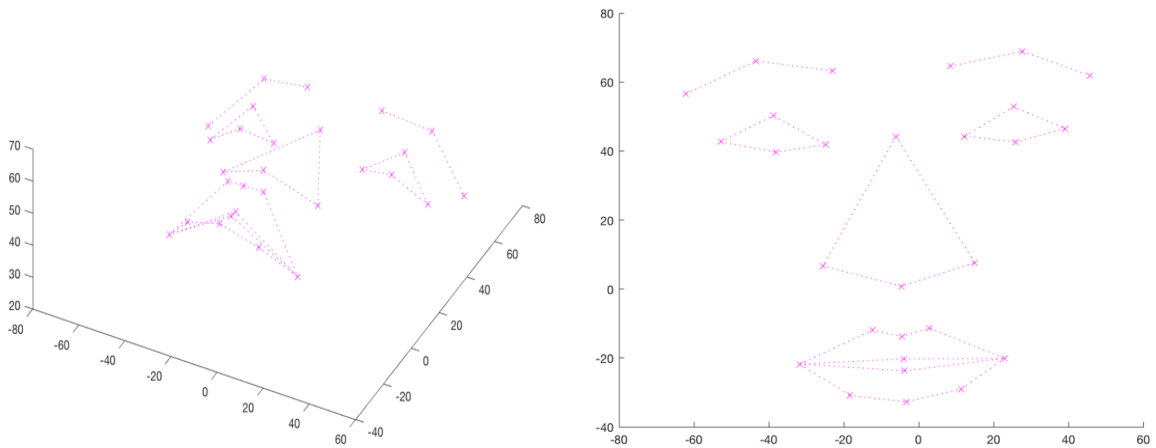

Figure 28: landmark average of 10 individual samples at time point T4 while smiling movement was being made: "The Average smiling face model at T4"
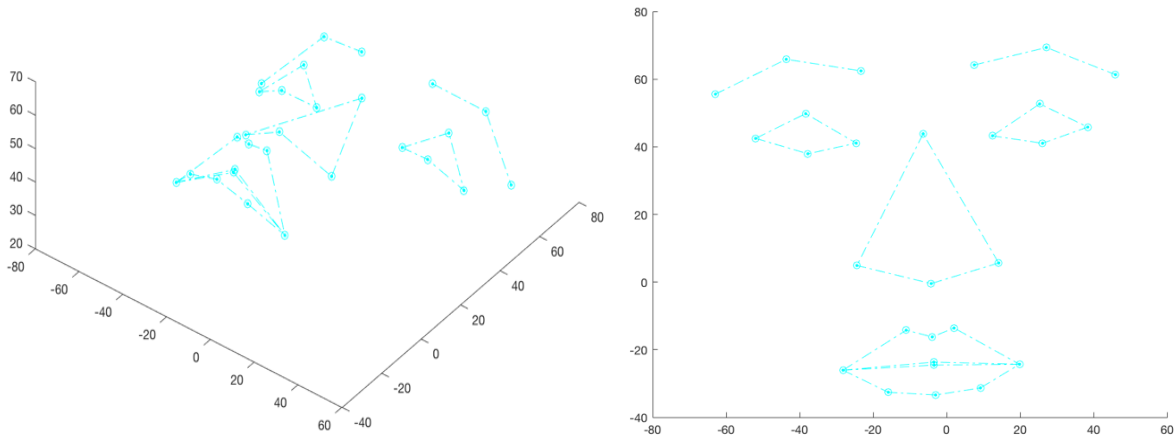
Figure 29: landmark average of 10 individual samples at time point T5 while smiling movement was being made: "The Average smiling face model at T5"

D. Computation of average displacement vectors and p values in three dimension & generation of color-coded displacement maps (p maps) during smiling movement between each time point

After development of the average smiling face models of the final 10 samples over five different time points, average displacement vectors were computed between each time point. All averaged landmarks are statistical points, and therefore not only displacement vectors themselves but also statistical p values were needed to be carefully investigated to see if which landmarks showed significant levels of movement during smiling facial expression and between which time point significant levels of movements occurred on those landmarks.

For more accurate computations of p values in three dimensions, a new approach has been developed by switching the coordinate system from the Cartesian coordinate to Spherical coordinate where distributive radii of all landmarks at each different time point in are used as random variables in this new system. Based on this new approach, new p values in three dimensions of all landmarks between each time point were computed via. paired sample t-test at the 5% significance level ($\alpha = 0.05$).

After computing p values of all landmarks in three dimension between each time point, colorized displacement vector p maps were generated, where threshold values were set to classify the significance level of displacement occurred at each landmark between each time point. The color schematic that we chose to represent significance in displacement was as follows: red represents severely significant displacement (p <0.01); yellow represents significant displacement (0.05<p<0.01); blue represents insignificant displacement (p>0.05).
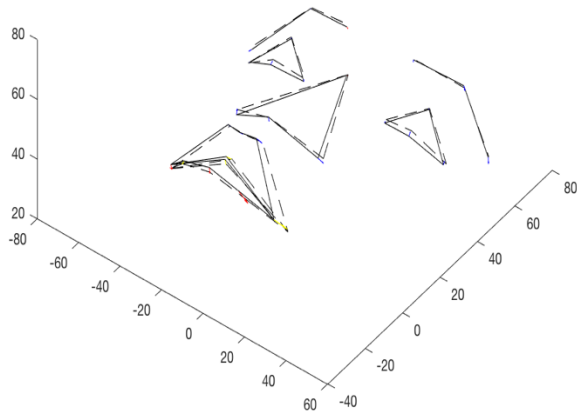
Having computed average displacement vectors and p values in 3D, color-coded displacement vector maps (p maps) between each time point were generated (Figure 30,31,32,33). In the color-coded displacement vector p maps, each averaged point will have directional vector where the length of the vector represents the magnitude of displacement, arrow of the vector shows the direction of the displacement, and the color of the vector will indicate the significance level of the movement of the landmark.

Corner of lip showed maximum displacement of 6.42 mm (p<~ 0.01) in upward and outward directions. Statistically significantly displacements were shown at oral region mostly (p<0.05) than nasal, eye, or eyebrow regions.
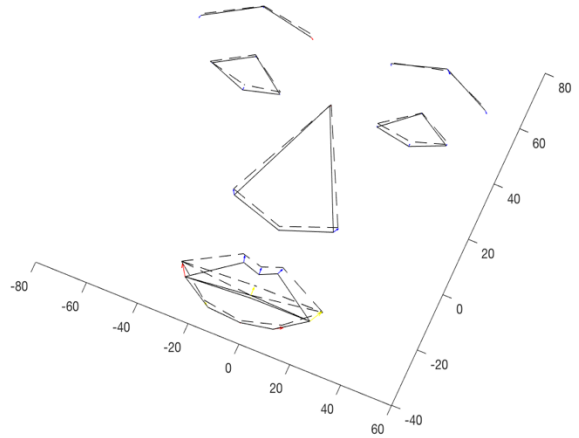
(a)

(b)

(c)

50
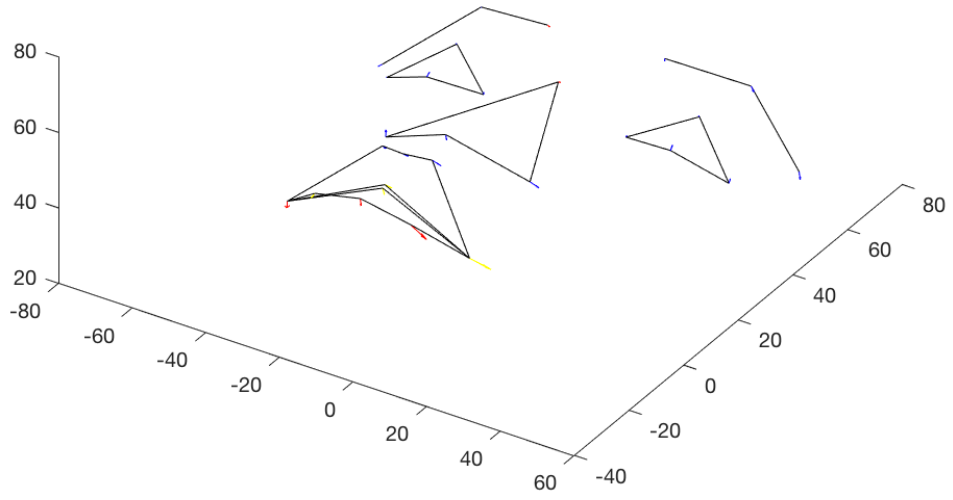
Figure 30: (a) Color-coded average displacement vector p map between T_1 and T_2 with average smiling face model at T_1 shown (b)(c) average smiling face models at T1 and T2 are shown with color-coded avg. p map, showing smiling trajectory between T1 and T2 (T1: solid line, T2: dashed line) (Severely significant (p<0.01, red), significant (0.05<p<0.01, yellow), and insignificant (p>0.05, blue).
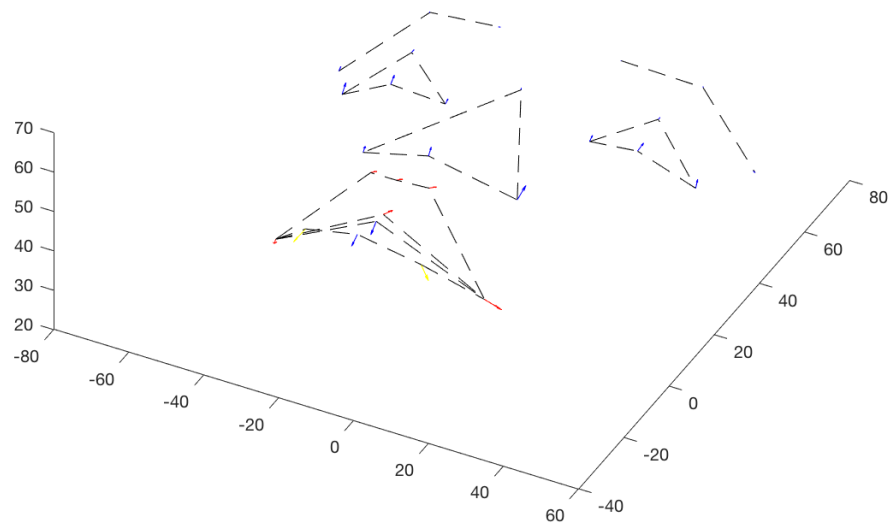
(a)

(b)

(c)

Figure 31: (a) Color-coded average displacement vector p map between T_2 and T_3 with average smiling face model at T_2 shown (b)(c) average smiling face models at T_2 and T_3 are shown with color-coded avg. p map, showing smiling trajectory between T_2 and T_3 (T_2: dashed line, T_3: dashdot line) (Severely significant ($p<0.01$, red), significant ($0.05<p<0.01$, yellow), and insignificant ($p>0.05$, blue).
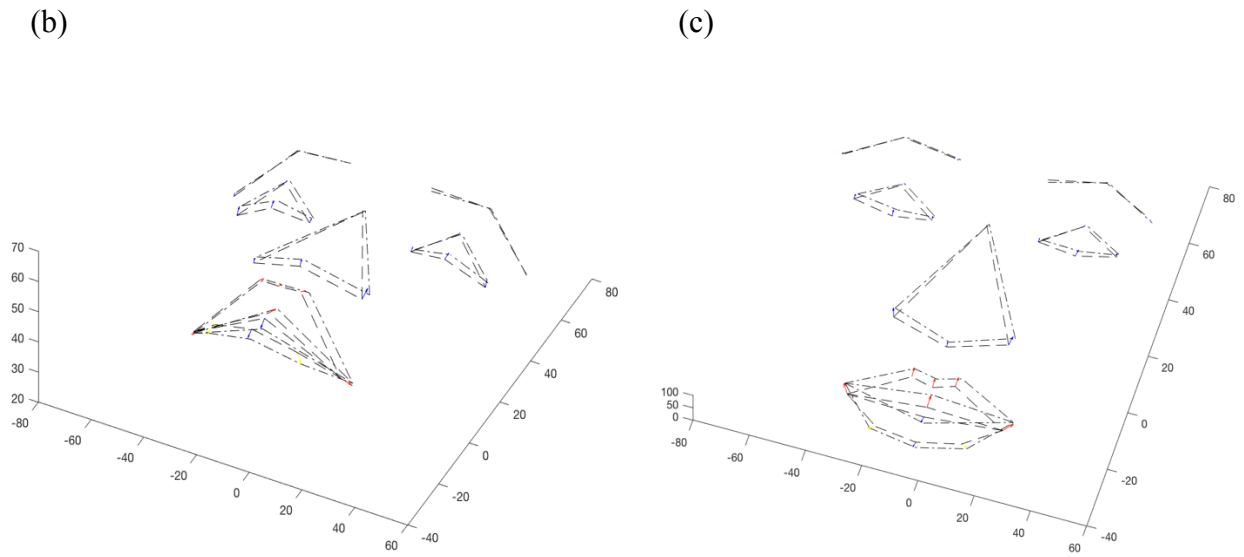
(a)

(b)

(c)

53

Figure 32: (a) Color-coded average displacement vector p map between T₃ and T₄ with average smiling face model at T₃ shown (b)(c) average smiling face models at T₃ and T₄ are shown with color-coded avg. p map, showing smiling trajectory between T₃ and T₄ (T₃: dashdot line, T₄: dotted line) (Severely significant (p<0.01, red), significant (0.05<p<0.01, yellow), and insignificant (p>0.05, blue).

(a)

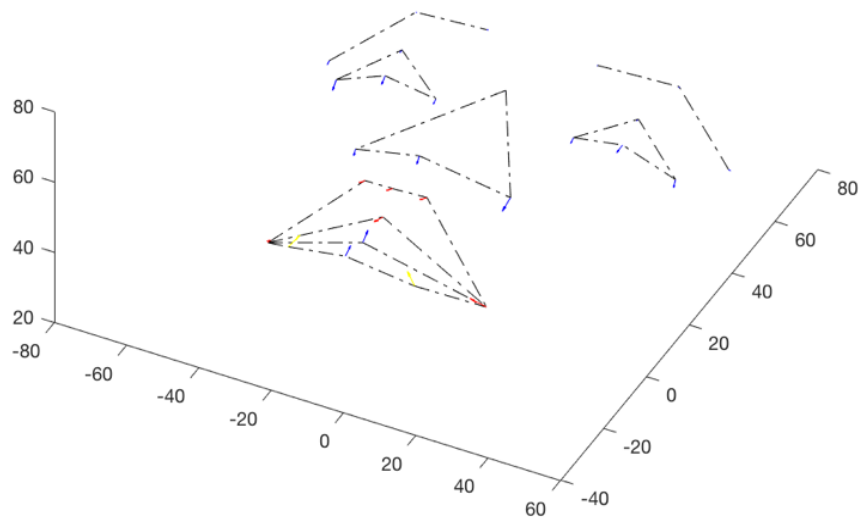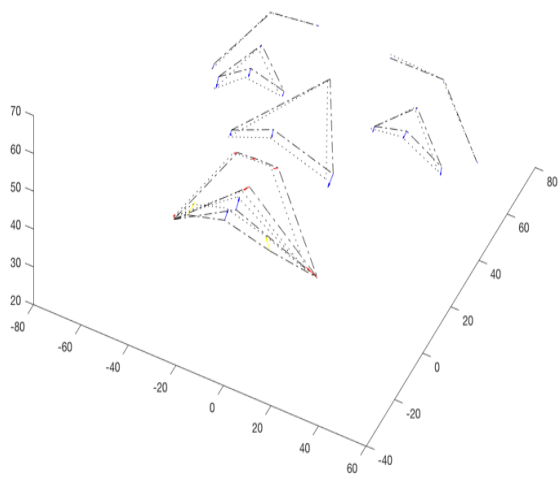(b)   (c)
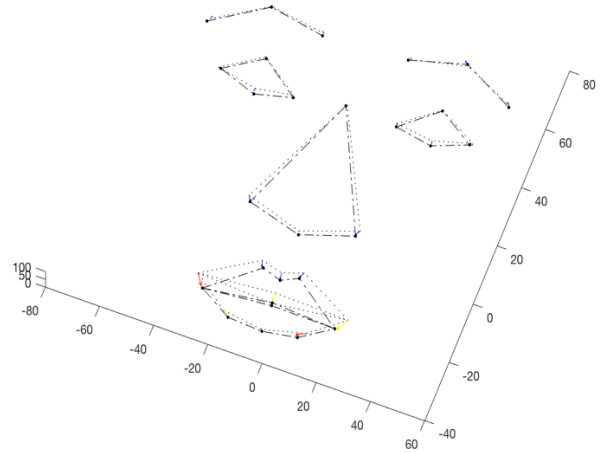
Figure 33: (a) Color-coded average displacement vector p map between T$_4$ and T$_5$ with average smiling face model at T$_4$ shown (b)(c) average smiling face models at T$_4$ and T$_5$ are shown with color-coded avg. p map, showing smiling trajectory between T$_4$ and T$_5$ (T$_4$: dotted line, T$_5$: dashdotdot line) (Severely significant (p<0.01, red), significant (0.05<p<0.01, yellow), and insignificant (p>0.05, blue).
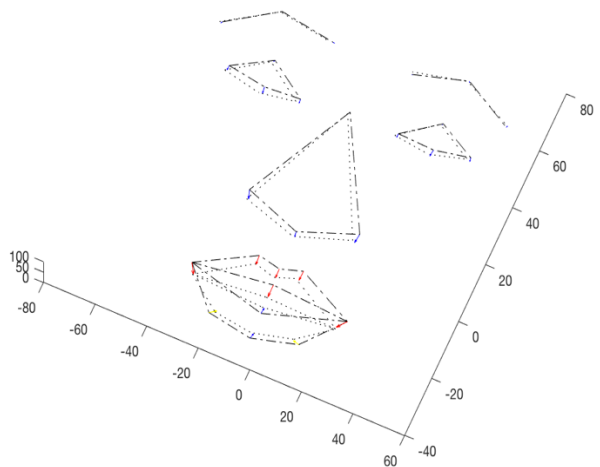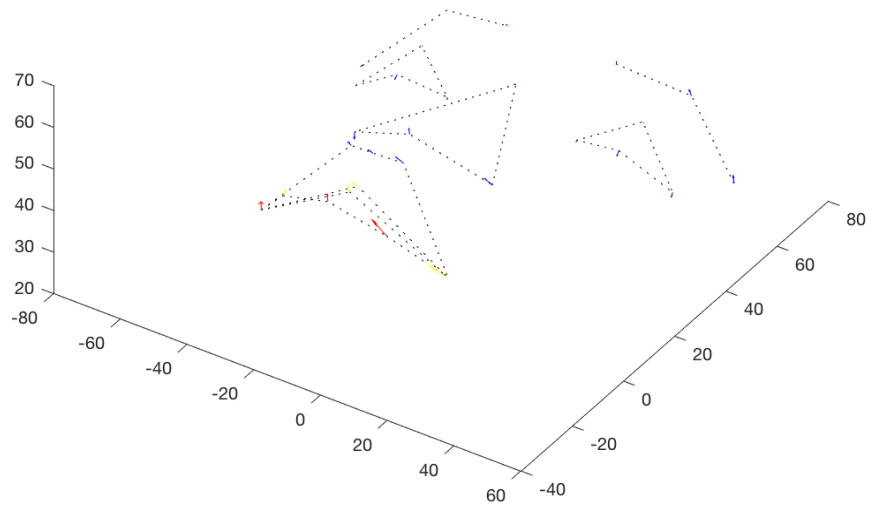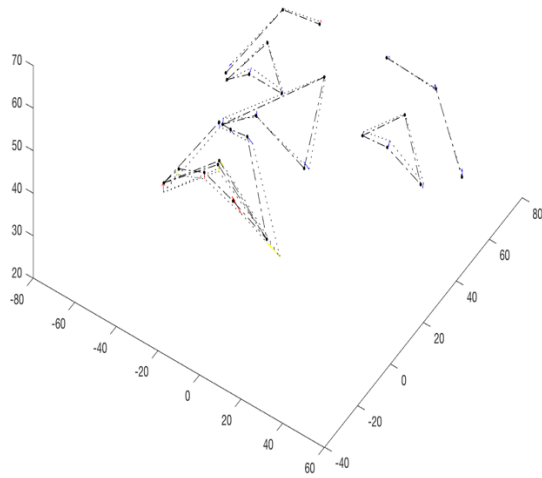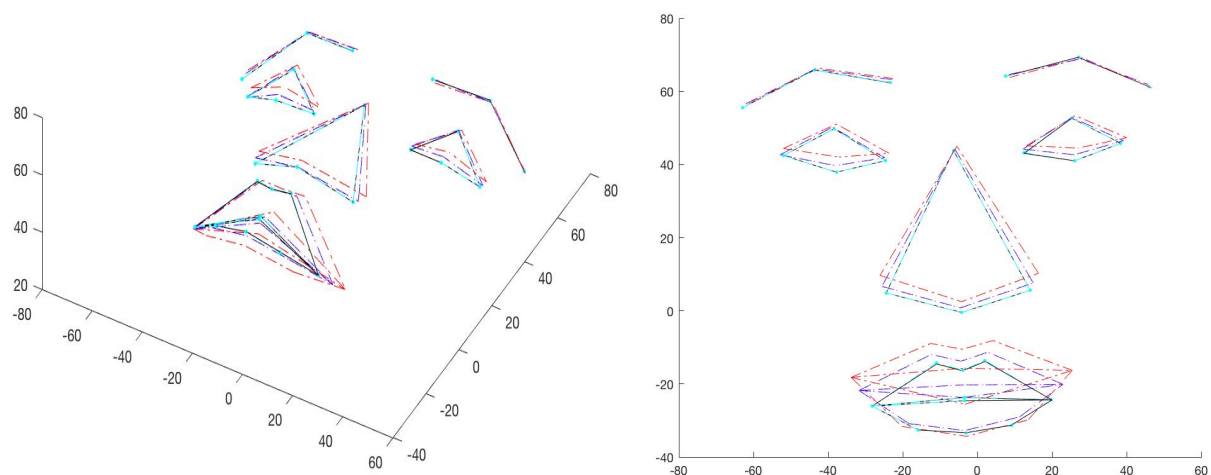
Figure 34: Average smiling face model at each time point T1,T2,T3,T4, and T5 was shown simultaneously to show trajectories of smiling movement (Animation of the average smiling movement trajectories over time will be presented during thesis defense) (Here, the average smiling face model at T1 in black, T2 in blue, T3 in red, T4 in magenta, and T5 in cyan).

Discussion

A) Clinical Applications

Our goal of this project was to successfully develop the method which could quantify the dynamic 3D movements of soft tissues while facial expressions are being made, opening a new door to the 3D dynamic analysis, seeking to advance static 3D imaging analysis into dynamic 3D movement analysis, adding another dimension to the diagnosis and treatment planning of patients

3dMD 3D facial models were taken of subjects from starting of facial expression till the end at five different time points, i.e., T_1, T_2, T_3, T_4, T_5 while facial expression was being made (T1: Neutral/Resting, T2: Mid-way through smile/frown/etc., T3: Complete smile/frown/etc., T4: Mid-way back to resting position, T5: Neutral/Resting). Since our investigation is the development of the 3D dynamic analysis protocol for the first time, formulations of homogenous facial expression samples were needed, resulting in classification of facial expression patterns. Homogenous 3dMD face models were aligned via establishment of vertex correspondence, and the landmarking process was complete.

We could successfully develop the averaging smiling face models at five different time points. After development of the average smiling face models from the final 10 samples over five different time points, average displacement vectors were computed between different time point, i.e., between T1 and T2, T2 and T3, T3 and T4, T4 and T5 in MATLAB, producing the average displacement for smiling movement. A new approach was developed to compute more accurate p values in 3 dimensions, by switching the coordinate system from the Cartesian coordinate to Spherical coordinate where distributive radii of all landmarks at each different time point were used as random variables in this new system.

Then, color-coded displacement vector p maps between each time point were generated, which could demonstrate the movements of each landmark but also how significant the movement of each landmark was by color-coding based on new p values in 3d dimensions. Therefore, magnitudes, directions, and significance of displacements of each landmark between each time point could be

quantitatively tracked and analyzed. Corner of lip showed maximum displacement of 6.42 mm ($p <\sim 0.01$) in upward and outward directions. Statistically significantly displacements were shown at oral region mostly ($p < 0.05$) than nasal, eye, or eyebrow regions.

To our knowledge, there have been no studies investigating in how to quantitatively analyze the dynamic movements of soft tissue in three dimension during various facial expressions. This is the first study to demonstrate that dynamic 3D movements of facial expressions can be quantitatively tracked and analyzed. This first new approach can offer an added dimension to the diagnosis and treatment planning of patients in the health care field.

Application of this new method would allow dynamic soft tissue movement (facial expressions) diagnostics for treatment planning in various health care specialties (i.e. orthodontics, oral/maxillofacial and plastic surgery). This would dramatically change the diagnostic paradigms currently used in craniofacial analysis (2D static facial analysis) towards a totally new and progressive direction.

Potential applications would be 1) generation of normative facial expression patterns across various strata, 2) quantification of treatment effect on facial expression pattern by comparing the average 4D models between T1 and T2, 3) comparison of facial expression patterns between patients with cleft lip/palate and a normative facial expression patterns, and 4) virtual patient creation (currently, we are confined to surface level(shell); by adding muscle mechanics inside soft tissue shell, we can create virtual soft tissue movement and predict those deformations of soft tissue)

B) Limitations

Currently available system in UCLA orthodontics clinic is 3dMD which can not reduce time duration (step-size) below 5 seconds, and this could limit our dynamic analysis. More ideally, if we can capture 3dMD face models with very small step-size, then this will reduce errors in Euler's method used in this research. It is also known that too large step-size could make the system unstable. There is a better method to improve system by varying step-size over the course of analysis. Whenever we can make step-size large without incurring too much error, we should do so, and when step-size has to be reduced to avoid excessive error, we want to do that also. However, in my project, step-size could not be adjusted over time due to the limitations of the 3dMD system we have.

C) Conclusions/Future directions

This project is the first study to demonstrate that dynamic 3D movements of facial expressions can be quantitatively tracked and analyzed. This will allow for the total paradigm shift from the 2D static facial analysis which has been used in health care system especially in our orthodontics field into 3D dynamic facial analysis.

Nowadays, advances in medial imaging open new perspectives for the improvement of patient diagnosis and treatment planning where biomechanical modeling of soft tissue and facial

expressions are necessary. One example is computer assisted surgery planning (CAS). In CAS, generation of the virtual model of a patient which can allow simulation of physical interactions with virtual bodies is important. Once the virtual model of a patient is generated, various case scenarios of the surgical impact and their outcomes can be extensively studied. Here, realistic simulation of soft tissue deformations under the impact of external forces is very important, and realistic prediction of the patient's post-operative appearance is an important feature of the planning system giving the surgeon unique feedback already during the planning stage [9].

However, challenges are complexity of soft tissue behavior. Most importantly, for the simulation of individual facial expressions, a correct biomechanical model of contracting muscles and their interaction with remaining facial tissue is needed.

In my research project, we were looing at the superficial points on the epidermis (facial surface), however, to fully understand the movement of those points, investigating the underlying structures below those points especially muscles are needed which are driving forces for the movements of those facial points. In building biomechanical models of contracting muscles, a model with a few dynamic parameters that emulate the primary characteristics is needed. Muscle themselves are grouped together to perform specific tasks. With all the muscle forms it is evident that they have a highly complex three-dimensional structure endowed with viscous, elastics and other mechanical properties that result in the displacement of the skin. Elasticity of the skin varies with age; young skin has a higher elasticity than older flesh and this factor should be accommodated in the muscle model [9]. Once biomechanical models of contracting muscles are built, then these can be combined with my quantitative analysis of the dynamic movements of facial soft tissue in 3D during facial expressions, moving towards the creation of a virtual patient.

References

1. Ekman P, Rosenberg EL. What the face reveals: basic and applied studies of spontaneous expression using the facial action coding system (FACS). New York: Oxford University Press; 1997.

2. Rubin LR, Rubin LR. The Anatomy Of A Smile. Plastic and Reconstructive Surgery. 1974;53(4):384–7.

3. Philips E. The Classification of Smile Patterns. J Can Dent Assoc. 65(5):252–4.

4. Jones S, Martin RD, Pilbeam DR. The Cambridge encyclopedia of human evolution. Cambridge: Cambridge University Press; 1992.

5. Hoque ME, Mcduff DJ, Picard RW. Exploring Temporal Patterns in Classifying Frustrated and Delighted Smiles. IEEE Transactions on Affective Computing. 2012;3(3):323–34.

6. Mcduff D, Kaliouby RE, Senechal T, Amr M, Cohn JF, Picard R. Affectiva-MIT Facial Expression Dataset (AM-FED): Naturalistic and Spontaneous Facial Expressions Collected "In-the-Wild" 2013 IEEE Conference on Computer Vision and Pattern Recognition Workshops. 2013;

7. Hadlock TA, Urban LS. Toward a Universal, Automated Facial Measurement Tool in Facial Reanimation. Archives of Facial Plastic Surgery. 2012Jan;14(4).

8. Paletz JL, Manktelow RT, Chaban R. The Shape of a Normal smile. Plastic and Reconstructive Surgery. 1994;93(4):784–9.

9. Gladilin E, Zachow S, Deuflhard P, Hege H-C. A biomechanical model for soft tissue simulation in craniofacial surgery. Proceedings International Workshop on

Medical Imaging and Augmented Reality.

10. L. F. Andrews and W. A. Andrews, Syllabus of the Andrews Orthodontic Philosophy, 9th ed. ed., San Diego, California: Lawrence F. Andrews, 2001.

11. Sarver DM. The importance of incisor positioning in the esthetic smile: The smile arc. American Journal of Orthodontics and Dentofacial Orthopedics. 2001;120(2):98–111.

12. Proffit WR, Fields HW. Contemporary orthodontics. 4th ed. Vol. 67. St. Louis: Mosby; 2007.

13. Gjørup H, Athanasiou AE. Soft-tissue and dentoskeletal profile changes associated with mandibular setback osteotomy. American Journal of Orthodontics and Dentofacial Orthopedics. 1991;100(4):312–23.

14. Johnston C, Burden D, Kennedy D, Harradine N, Stevenson M. Class III surgical-orthodontic treatment: A cephalometric study. American Journal of Orthodontics and Dentofacial Orthopedics. 2006;130(3):300–9.

15. Hu J, Wang D, Luo S, Chen Y. Differences in soft tissue profile changes following mandibular setback in chinese men and women. Journal of Oral and Maxillofacial Surgery. 1999;57(10):1182–6.

16. Enacar A, Taner T, Toroglu S. Analysis of soft tissue profile changes associated with mandibular setback and double-jaw surgeries. International Journal of Adult Orthodontics and Orthognathic Surgery. 1999;14:27–35.

17. McCance A, Moss J, Fright W, James D, Linney A. A three dimensional analysis of soft and hard tissue changes following bimaxillary orthognathic surgery in skeletal III patients. British Journal of Oral and Maxillofacial Surgery. 1992;30(5):305–12.

18. Ozsoy U, Demirel BM, Yildirim FB, Tosun O, Sarikcioglu L. Method selection in

craniofacial measurements: Advantages and disadvantages of 3D digitization method. Journal of Cranio-Maxillofacial Surgery. 2009;37(5):285–90.

19. Ghoddousi H, Edler R, Haers P, Wertheim D, Greenhill D. Comparison of three methods of facial measurement. International Journal of Oral and Maxillofacial Surgery. 2007;36(3):250–8.

20. Cavalcanti M, Rocha S, Vannier M. Craniofacial measurements based on 3D-CT volume rendering: implications for clinical applications. Dentomaxillofacial Radiology. 2004;33(3):170–6.

21. Kim N-K, Lee C, Kang S-H, Park J-W, Kim M-J, Chang Y-I. A three-dimensional analysis of soft and hard tissue changes after a mandibular setback surgery. Computer Methods and Programs in Biomedicine. 2006;83(3):178–87.

22. McComb R. An Exploratory Approach for Mapping the Surface of the Human Skull in Three Dimensions: Technical Methods and Clinical Application. 2012;

23. Lee Y, Terzopoulos D, Walters K. Realistic modeling for facial animation. Proceedings of the 22nd annual conference on Computer graphics and interactive techniques - SIGGRAPH '95. 1995;

24. Geerts F. Moving Objects and Their Equations of Motion. Constraint Databases Lecture Notes in Computer Science. 2004;:40–51.

25. Siqueira FDL, Bogorny V. Discovering Chasing Behavior in Moving Object Trajectories. Transactions in GIS. 2011;15(5):667–88.

26. Chen Y, Jiang S, Ooi BC, Tung AK. Querying Complex Spatio-Temporal Sequences in Human Motion Databases. 2008 IEEE 24th International Conference on Data Engineering. 2008;

27. Güting RH, Böhlen MH, Erwig M, Jensen CS, Lorentzos NA, Schneider M, et al. A

foundation for representing and querying moving objects. ACM Transactions on Database Systems. 2000Jan;25(1):1–42.

28. Sun Y, Chen X, Rosato M, Yin L. Tracking Vertex Flow and Model Adaptation for Three-Dimensional Spatiotemporal Face Analysis. IEEE Transactions on Systems, Man, and Cybernetics - Part A: Systems and Humans. 2010;40(3):461–74.

29. Pixar Research - Physically Based Modeling [Internet]. Pixar Research - Physically Based Modeling. [cited 2017Jan15]. Available from: http://www.pixar.com/companyinfo/research/pbm2001/index.html

30. Arnolʹd VI. Mathematical methods of classical mechanics. New York, NY: Springer New York; 2010.

31. Feynman RP, Leighton RB, Sands M. The Feynman lectures on physics. New York, NY: Basic Books; 2010.

32. Iserles A. A first course in the numerical analysis of differential equations. Cambridge: Cambridge University Press; 1996.

33. Newton I. Philosophiae naturalis principia mathematica. Londini: Jussu Societatis Regiæ ac Typis Josephi Streater. Prostat apud plures Bibliopolas.; 1687.

34. Chiu C, Clark R. Reproducibility of natural head position. Journal of Dentistry. 1991;19(2):130–1.

35. Solow B, Tallgren A. Natural Head Position in Standing Subjects. Acta Odontologica Scandinavica. 1971;29(5):591–607.

36. Lundstrom A, Lundstrom F, Lebret LML, Moorrees CFA. Natural head position and natural head orientation: basic considerations in cephalometric analysis and research. The European Journal of Orthodontics. 1995Jan;17(2):111–20.

37. Gor T, Kau CH, English JD, Lee RP, Borbely P. Three-dimensional comparison of

facial morphology in white populations in Budapest, Hungary, and Houston, Texas. American Journal of Orthodontics and Dentofacial Orthopedics. 2010;137(3):424–32.

38. Kau CH, Richmond S, Zhurov AI, Knox J, Chestnutt I, Hartles F, et al. Reliability of measuring facial morphology with a 3-dimensional laser scanning system. American Journal of Orthodontics and Dentofacial Orthopedics. 2005;128(4):424–30.

39. Alashkar T, Amor BB, Daoudi M, Berretti S. A Grassmannian Framework for Face Recognition of 3D Dynamic Sequences with Challenging Conditions. Computer Vision - ECCV 2014 Workshops Lecture Notes in Computer Science. 2015;:326–40.

40. Bettadapura V. Face expression recognition and analysis: the state of the art . 2012;

41. Wang Y, Huang X, Lee C-S, Zhang S, Li Z, Samaras D, et al. High Resolution Acquisition, Learning and Transfer of Dynamic 3-D Facial Expressions. Computer Graphics Forum. 2004;23(3):677–86.

42. Ekman P, Friesen WV. Facial action coding system. Palo Alto, CA: Consulting Psychologists Press; 1978.

43. How Can Facial Expressions Help You Read Employees? [Internet]. How Can Facial Expressions Help You Read Employees? |. [cited 2017Jan15]. Available from: http://blog.tnsemployeeinsights.com/how-can-facial-expressions-help-you-read-employees/

44. Humintell [Internet]. Humintell RSS. [cited 2017Jan15]. Available from: http://www.humintell.com/macroexpressions-microexpressions-and-subtle-expressions/

45. Ekman P. Conclusion: What We Have Learned by Measuring Facial Behavior: Further Comments and Clarifications. What the Face RevealsBasic and Applied

Studies of Spontaneous Expression Using the Facial Action Coding System (FACS). 2005;:605–26.

46. Roberts A. Curvature attributes and their application to 3D interpreted horizons. First Break. 2001;19(2):85–100.

47. Chen J. Automatic Face Animation with Linear Model. 2008;

48. D'agostino E, Maes F, Vandermeulen D, Suetens P. A viscous fluid model for multimodal non-rigid image registration using mutual information. Medical Image Analysis. 2003;7(4):565–75.

49. Maes F, Collignon A, Vandermeulen D, Marchal G, Suetens P. Multi-modality image registration by maximization of mutual information. Proceedings of the Workshop on Mathematical Methods in Biomedical Image Analysis. 1996;

50. Rueckert D, Sonoda L, Hayes C, Hill D, Leach M, Hawkes D. Nonrigid registration using free-form deformations: application to breast MR images. IEEE Transactions on Medical Imaging. 1999;18(8):712–21.

51. Wu J, Tse R, Shapiro LG. Automated face extraction and normalization of 3D Mesh Data. 2014 36th Annual International Conference of the IEEE Engineering in Medicine and Biology Society. 2014;

52. Shapiro LG, Wilamowska K, Atmosukarto I, Wu J, Heike C, Speltz M, et al. Shape-Based Classification of 3D Head Data. Image Analysis and Processing – ICIAP 2009 Lecture Notes in Computer Science. 2009;:692–700.

53. Waters K. A muscle model for animation three-dimensional facial expression. ACM SIGGRAPH Computer Graphics. 1987Jan;21(4):17–24.

54. Deng Z, Chiang P-Y, Fox P, Neumann U. Animating blendshape faces by cross-mapping motion capture data. Proceedings of the 2006 symposium on Interactive 3D

graphics and games - SI3D '06. 2006;

55. Bickel B, Botsch M, Angst R, Matusik W, Otaduy M, Pfister H, et al. Multi-scale capture of facial geometry and motion. ACM Transactions on Graphics. 2007;26(99):33.

56. Ekman P. Facial action coding system: investigator's guide. Palo Alto, CA: Consulting Psychologists Press; 1978.

57. Ekman P, Friesen WV, Hager JC. Facial action coding sytem. Salt Lake City, UT: A Human Face; 2002.

58. Clemente CD. Anatomy: a regional atlas of the human body. Baltimore: Williams & Wilkins; 1997.

59. Nanda V, Gutman B, Bar E, Alghamdi S, Tetradis S, Lusis AJ, et al. Quantitative analysis of 3-dimensional facial soft tissue photographic images: technical methods and clinical application. Progress in Orthodontics. 2015Jul2;16(1).

60. Pandzic IS. MPEG-4 Facial Animation Framework for the Web and Mobile Applications. MPEG-4 Facial Animation. :65–79.

61. Chang Y, Vieira M, Turk M, Velho L. Automatic 3D Facial Expression Analysis in Videos. Lecture Notes in Computer Science Analysis and Modelling of Faces and Gestures. 2005;:293–307.

62. Ackerman J, Proffit WR, Sarver DM. The emerging soft tissue paradigm in orthodontic diagnosis and treatment planning. Clin Orthod Res. 1999;2:49–52.